of the carbene bands and growth of bands assigned to alkene **12**. The band positions and intensities match closely those reported in the literature.[32] IR of **12** (argon matrix): 1784.8 (vs), 1321.9 (vs), 1221.6 (vs), 1199.6 (vs), 1071.4 (m), 1037.1 (s), 1020.0 (vs), 695.8 (w), 667.6 (w) cm^{-1}.

Matrix Isolation Spectra. UV. 3-Fluoro-3-(trifluoromethyl)diazirine (4). From a 1:480 mixture of diazirine **4** in argon, 130 Torr was deposited. UV (argon matrix): λ_{max} = 328, 313 nm. See also Results.

3-Chloro-3-(trifluoromethyl)diazirine (5). From a 1:250 mixture of diazirine **5** in argon, 180 Torr was deposited. UV (argon matrix): λ_{max} = 332, 318 nm. See also Results.

3-Bromo-3-(trifluoromethyl)diazirine (6). From a 1:200 mixture of diazirine **6** in argon, 190 Torr was deposited. UV (argon matrix): λ_{max} = 334, 320 nm. See also Results.

Fluoro(trifluoromethyl)carbene (1). Photolysis of matrix-isolated **4** at 12 K for 1.3 h (λ = 316 nm) resulted in complete loss of the diazirine absorptions and generation of two new absorptions assigned to carbene **1**. UV of **1** (argon matrix): λ_{max} = 465 ($\epsilon \approx 100$ (L cm^{-1})/mol), 230 nm. See also Results.

Chloro(trifluoromethyl)carbene (2). Photolysis of matrix-isolated **5** at 12 K for 1.5 h (λ = 318 nm) resulted in complete loss of the diazirine absorptions and generation of two new absorptions assigned to carbene **2**. UV of **2** (argon matrix): λ_{max} = 640 ($\epsilon \approx 60$ (L cm^{-1})/mol), 235 nm. See also Results.

Bromo(trifluoromethyl)carbene (3). Photolysis of matrix-isolated **6** at 12 K for 1.5 h (λ = 320 nm) resulted in complete loss in the diazirine absorptions and generation of two new absorptions assigned to carbene **3** in addition to a small band at 400 nm. Subsequent photolysis at 400 nm (15 min) completely destroyed the 400-nm absorption with no change in the remaining spectrum. UV of **3** (argon matrix): λ_{max} = 665 ($\epsilon \approx 45$ (L cm^{-1})/mol), 270 (sh), 235 nm. See also Results.

Acknowledgment. We are grateful to the National Science Foundation (Grant CHE-8822674) for support of this work and to Dr. George Furst for help with the FTIR. The Research Foundation at the University of Pennsylvania generously provided funds to upgrade the departmental FTIR facility. W.P.D. thanks the Alfred P. Sloan Foundation for a research fellowship (1990-1992).

Registry No. **1**, 58734-91-1; **2**, 22189-12-4; **3**, 139871-62-8; **4**, 117113-32-3; **5**, 58911-30-1; **6**, 117113-33-4; **7**, 2837-89-0; **8**, 306-83-2; **9**, 151-67-7; **10**, 116-14-3; **11**, 79-38-9; **12**, 598-73-2; **13**, 139871-63-9; **14**, 13453-52-6; **15**, 2108-20-5; **16**, 17141-28-5; HCl, 7047-01-0; N_2, 7727-37-9; trifluoroacetamidine, 354-37-0; (trifluoromethyl)diazomethane, 371-67-5; *tert*-butyl hypobromite, 1611-82-1; *cis*-perfluoro-2-butene, 1516-65-0; *trans*-perfluoro-2-butene, 1516-64-9.

(32) Mann, D. E.; Acquista, N.; Plyler, E. K. *J. Chem. Phys.* **1954**, *22*, 1199.

Triplet and Singlet Energy Transfer in Carotene-Porphyrin Dyads: Role of the Linkage Bonds

Devens Gust,* Thomas A. Moore,* Ana L. Moore,* Chelladurai Devadoss, Paul A. Liddell, Roel Hermant, Ronald A. Nieman, Lori J. Demanche, Janice M. DeGraziano, and Isabelle Gouni

Contribution from the Department of Chemistry and Biochemistry and Center for the Study of Early Events in Photosynthesis, Arizona State University, Tempe, Arizona 85287-1604.
Received October 17, 1991

Abstract: A series of carotenoporphyrin dyad molecules in which the carotenoid is covalently linked to a tetraarylporphyrin at the ortho, meta, or para position of a meso aromatic ring has been prepared, and the molecules have been studied using steady-state and transient fluorescence emission, transient absorption, and ^1H NMR methods. Triplet-triplet energy transfer from the porphyrin moiety to the carotenoid has been observed, as has singlet-singlet energy transfer from the carotenoid polyene to the porphyrin. In addition, the carotenoid quenches the fluorescence of the attached porphyrin by a mechanism which increases internal conversion. The rates of all three of these processes are slower for the meta isomer than for the corresponding ortho and para molecules. Analysis of the data suggests that the triplet-triplet energy transfer is mediated by a through-bond (superexchange) mechanism involving the π-electrons of the linkage bonds, rather than a direct, through-space coupling of the chromophores. The same appears to be true for the process leading to enhanced internal conversion. The results are consistent with a role for the through-bond mechanism in the singlet-singlet energy transfer as well. Simple Hückel molecular orbital calculations are in accord with the proposed through-bond process.

Photochemical interactions between carotenoid polyenes and closely associated cyclic tetrapyrroles are important aspects of photosynthesis. For example, carotenoids provide photoprotection by rapidly quenching chlorophyll triplet states which are formed in antenna systems or photosynthetic reaction centers. This triplet-triplet energy transfer prevents chlorophyll-sensitized production of singlet oxygen, which is injurious to the organism.[1-6] In addition, carotenoids act as antennas by absorbing light in spectral regions where chlorophyll absorbs weakly and delivering the resulting excitation to chlorophyll via a singlet-singlet energy-transfer process.[7-11] Finally, chlorophyll first excited singlet states are quenched by nearby carotenoids.[12-14] This quenching has been ascribed to energy transfer,[15] or to electron transfer[12]

(1) Griffiths, M.; Sistrom, W. R.; Cohen-Bazire, G.; Stanier, R. Y. *Nature* **1955**, *176*, 1211.
(2) Cohen-Bazire, G.; Stanier, R. Y. *Nature* **1958**, *181*, 250.
(3) Foote, C. S.; Denny, R. W. *J. Am. Chem. Soc.* **1968**, *90*, 6233.
(4) Foote, C. S.; Chang, Y. C.; Denny, R. W. *J. Am. Chem. Soc.* **1970**, *92*, 5216.
(5) Monger, T. G.; Cogdell, R. J.; Parson, W. W. *Biochim. Biophys. Acta* **1976**, *449*, 136.
(6) Davidson, E.; Cogdell, R. J. *Biochim. Biophys. Acta* **1981**, *635*, 295.
(7) Goedheer, J. D. *Biochim. Biophys. Acta* **1969**, *172*, 252.
(8) Bazzaz, M. B.; Govindjee *Plant Physiol.* **1973**, *52*, 257.
(9) Cogdell, R. J.; Hipkins, M. F.; MacDonald, W.; Truscott, T. G. *Biochim. Biophys. Acta* **1981**, *634*, 191.
(10) Cogdell, R. J.; Frank, H. A. *Biochim. Biophys. Acta* **1987**, *895*, 63.
(11) Sauer, K. *Acc. Chem. Res.* **1978**, *11*, 257.
(12) Beddard, G. S.; Davidson, R. S.; Trethewey, K. R. *Nature* **1977**, *267*, 373.
(13) Gust, D.; Moore, T. A.; Liddell, P. A.; Nemeth, G. A.; Makings, L. R.; Moore, A. L.; Barrett, D.; Pessiki, P. J.; Bensasson, R. V.; Rougée, M.; Chachaty, C.; De Schryver, F. C.; Van der Auweraer, M.; Holzwarth, A. R.; Connolly, J. S. *J. Am. Chem. Soc.* **1987**, *109*, 846.
(14) Moore, T. A.; Gust, D.; Hatlevig, S.; Moore, A. L.; Makings, L. R.; Pessiki, P. J.; De Schryver, F. C.; Van der Auweraer, M.; Lexa, D.; Bensasson, R. V.; Rougée, M. *Isr. J. Chem.* **1988**, *28*, 87.

0002-7863/92/1514-3590$03.00/0

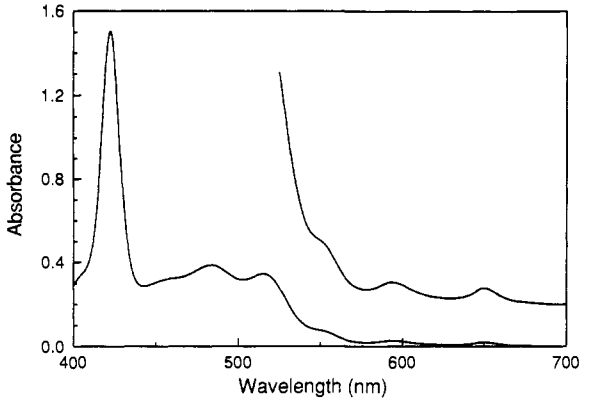

Figure 1. Absorption spectrum of carotenoporphyrin **1** in toluene solution. The inset is multiplied by a factor of 4 in absorbance.

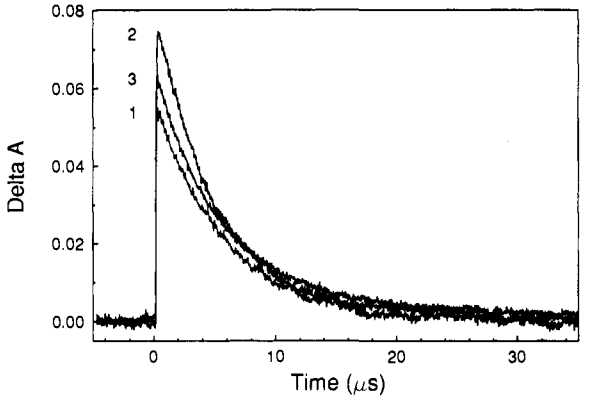

Figure 2. Decay of the carotenoid triplet state absorption at 550 nm of 3×10^{-5} M solutions of carotenoporphyrins **1–3** following excitation with a 650-nm laser pulse. Data were taken at a rate of 40 ns per point. The ΔA values ($\epsilon_T - \epsilon_G$) for the three curves are for samples with equal absorbance at the pump wavelength.

or some other process leading to internal conversion, and may play a role in the regulation of photosynthesis.[16]

Synthetic multicomponent molecules which demonstrate these same photochemical processes have been prepared and studied. In our laboratories, porphyrins and chlorophyll derivatives have been covalently linked to carotenoids in order to mimic carotenoid photoprotection[17-26] and antenna function.[17,18,20,21,23,25,27-29] Many of these molecules also feature quenching of the tetrapyrrole fluorescence. A number of carotenoid-containing artificial reaction centers which are designed to model the photoinitiated production of long-lived, energetic charge separated states characteristic of natural photosynthesis also exhibit the same three photochemical phenomena.[17,30,31]

The importance of these processes in natural and artificial photosynthesis prompted us to undertake an examination of the mechanisms by which they occur. To that end, we have prepared carotenoporphyrin dyads **1**, **2**, and **3**. These molecules differ only in that the carotenoid moiety is covalently linked to a porphyrin aryl ring via amide groups para, meta, and ortho to the porphyrin macrocycle, respectively. Dyads **4** and **5**, in which the carotenoid is linked to the porphyrin aryl ring via reversed amide linkages, have also been synthesized. Porphyrin-to-carotenoid triplet–triplet

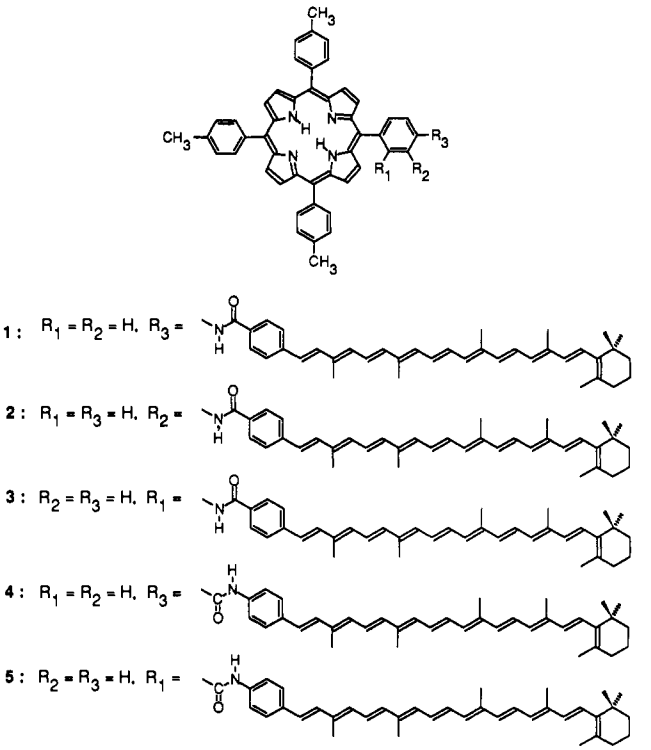

energy transfer in these molecules was studied using transient absorption spectroscopy on the nanosecond time scale. Singlet–singlet energy transfer from carotenoid to porphyrin was investigated using fluorescence excitation spectroscopy, whereas porphyrin fluorescence quenching was detected via time-resolved fluorescence spectroscopy. Finally, the conformational preferences of the molecules were investigated using ^{1}H NMR and molecular mechanics methods.

Results

The porphyrin moieties were prepared by condensation of pyrrole and an appropriate mixture of aromatic aldehydes in propionic acid. The requisite carotenoid polyenes were prepared from 8′-apo-β-carotenal by means of a Wittig reaction and linked to the porphyrin via an acid chloride. The syntheses of the required compounds and their characterization with UV–vis, NMR, and mass spectrometric techniques are described in the Experimental Section.

Absorption Spectra. The absorption spectrum of carotenoporphyrin **1** in toluene solution is shown in Figure 1. The porphyrin Soret band is clearly evident at 422 nm, and three of the Q-bands can be discerned at 552, 593, and 650 nm. The fourth Q-band, which occurs at 517 nm in the isolated porphyrin, is obscured by the strong carotenoid absorptions at 459, 484, and 514 nm. The spectrum is essentially a linear combination of the

(15) Snyder, R.; Arvidson, E.; Foote, C.; Harrigan, L.; Christensen, R. L. *J. Am. Chem. Soc.* **1985**, *105*, 4117.
(16) Deming-Adams, B. *Biochim. Biophys. Acta* **1990**, *1020*, 1.
(17) Gust, D.; Moore, T. A. *Adv. Photochem.* **1991**, *16*, 1.
(18) Bensasson, R. V.; Land, E. J.; Moore, A. L.; Crouch, R. L.; Dirks, G.; Moore, T. A.; Gust, D. *Nature* **1981**, *290*, 329.
(19) Moore, A. L.; Joy, A.; Tom, R.; Gust, D.; Moore, T. A.; Bensasson, R. V.; Land, E. J. *Science* **1982**, *216*, 982.
(20) Moore, T. A.; Gust, D.; Mathis, P.; Mialocq, J.-C.; Chachaty, C.; Bensasson, R. V.; Land, E. J.; Doizi, D.; Liddell, P. A.; Lehman, W. R.; Nemeth, G. A.; Moore, A. L. *Nature* **1984**, *301*, 630.
(21) Gust, D.; Moore, T. A. *J. Photochem.* **1985**, *29*, 173.
(22) Gust, D.; Moore, T. A.; Bensasson, R. V.; Mathis, P.; Land, E. J.; Chachaty, C.; Moore, A. L.; Liddell, P. A.; Nemeth, G. A. *J. Am. Chem. Soc.* **1985**, *107*, 3631.
(23) Liddell, P. A.; Barrett, D.; Makings, L. R.; Pessiki, P. J.; Gust, D.; Moore, T. A. *J. Am. Chem. Soc.* **1986**, *108*, 5350.
(24) Frank, H. A.; Chadwick, B. W.; Oh, J. J.; Gust, D.; Moore, T. A.; Liddell, P. A.; Moore, A. L.; Makings, L. R.; Cogdell, R. J. *Biochim. Biophys. Acta* **1987**, *892*, 253.
(25) Moore, T. A.; Gust, D.; Moore, A. L. In *Carotenoids: Chemistry and Biology*; Krinsky, N. I., Mathews-Roth, M. M., Taylor, R. F., Ed.; New York: Plenum Press, 1989; pp 223.
(26) Liddell, P. A.; Nemeth, G. A.; Lehman, W. R.; Joy, A. M.; Moore, A. L.; Bensasson, R. V.; Moore, T. A.; Gust, D. *Photochem. Photobiol.* **1982**, *36*, 641.
(27) Dirks, G.; Moore, A. L.; Moore, T. A.; Gust, D. *Photochem. Photobiol.* **1980**, *32*, 277.
(28) Moore, A. L.; Dirks, G.; Gust, D.; Moore, T. A. *Photochem. Photobiol.* **1980**, *32*, 691.
(29) Wasielewski, M. R.; Liddell, P. A.; Barrett, D.; Moore, T. A.; Gust, D. *Nature* **1986**, *322*, 570.
(30) Gust, D.; Moore, T. A. *Top. Curr. Chem.* **1991**, *159*, 103.
(31) Gust, D.; Moore, T. A. *Science* **1989**, *244*, 35.

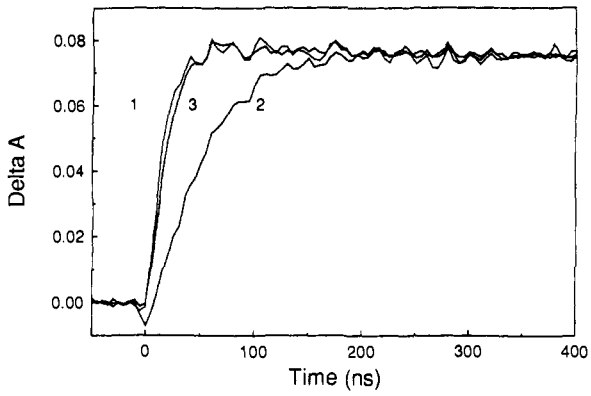

Figure 3. Rise of the carotenoid triplet state absorption at 550 nm of 3 × 10^{-5} M solutions of carotenoporphyrins **1–3** following excitation with a 650-nm laser pulse. Data were taken at a rate of 5 ns per point. The ΔA values have been normalized at long times in order to illustrate the difference in growth rates. The absorbance for **1** and **3** rises with the instrument response, but that of **2** increases with a time constant of 40 ns.

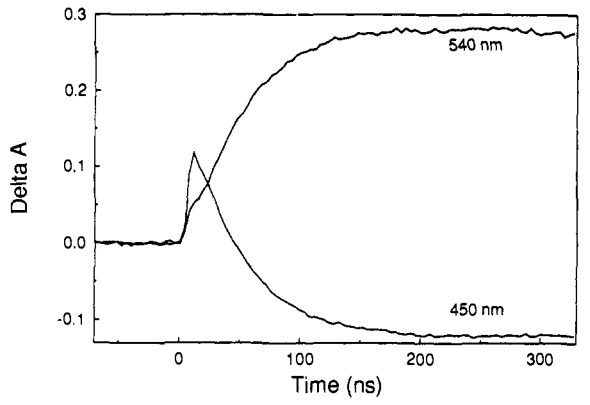

Figure 4. Rise of the carotenoid triplet state absorption at 550 nm and concomitant decay of the porphyrin triplet state absorption at 450 nm following excitation of a toluene solution of **2** with a 650-nm, 5-ns laser pulse. The porphyrin triplet absorption decays into the carotenoid ground-state bleach resulting from the population of the carotenoid triplet state.

absorption spectra of unlinked porphyrin and carotenoid model systems; there is no evidence for strong interactions between the pigments which significantly perturb the absorption. The absorption spectra of **2–5** are similar to that shown for **1** (see the Experimental Section).

Triplet–Triplet Energy Transfer. Triplet–triplet energy transfer from porphyrins to carotenoids may be readily detected using transient absorption spectroscopy. The polyene triplet has an absorption maximum ($\epsilon_T - \epsilon_G$) at about 540 nm,[19,22] whereas the porphyrin triplet has a strong absorption at 440 nm.[22] Excitation of a 3 × 10^{-5} M solution of **1** in toluene, which had been deoxygenated by bubbling with argon, with a 650-nm, ca. 15-ns laser pulse led to the observation of a transient absorption at 550 nm. The decay of the transient is shown in Figure 2. (Similar results were obtained with a 590-nm excitation.) Although the 650-nm laser pulse excites only the porphyrin moiety, the 550-nm decay is characteristic of a carotenoid triplet state. The lifetime of this transient, 5.7 μs, is typical of carotenoid triplet states in deoxygenated solvents. Admission of oxygen to the sample reduced the lifetime of the transient. Since carotenoid triplet states are quenched by oxygen to yield two ground-state species with a rate constant about one-third that for diffusion, this result is consistent with the triplet nature of the transient. Thus, the carotenoid triplet state is formed as shown:

$$C\text{–}P \xrightarrow{h\nu} C\text{–}{}^1P \quad (1)$$

$$C\text{–}{}^1P \xrightarrow{k_{isc}} C\text{–}{}^3P \quad (2)$$

$$C\text{–}{}^3P \xrightarrow{k_{tt}} {}^3C\text{–}P \quad (3)$$

We have observed similar triplet–triplet energy transfer in a variety of other carotenoporphyrin systems.[17-22,24,25]

Excitation of **2** and **3** under the same conditions allows observation of similar transient absorptions at 550 nm, with similar lifetimes of 5.7 μs (Figure 2). Thus, triplet–triplet energy transfer is also occurring in these systems. However, solutions of **1**, **2**, and **3** having equal absorbances at the 650-nm pump wavelength produce different amounts of carotenoid triplet (Figure 2). The relative yield immediately after the laser pulse (40 ns/data point) is 0.74:1.00:0.84 for the para, meta, and ortho compounds (**1**, **2**, and **3**), respectively.

Examination of the 550-nm transient absorptions on a shorter time scale allows study of the rate of formation of the carotenoid triplet states. As shown in Figure 3, the (normalized) carotenoid triplet absorptions of **1** and **3** rise with the time resolution of the transient spectrometer. Thus, since porphyrin triplet states live for hundreds of micro- or milliseconds under similar conditions, k_{tt} for these molecules is greater than 1 × 10^8 s^{-1} and may approach or exceed k_{isc}. Meta isomer **2**, on the other hand, demonstrates a slower growth of the carotenoid triplet with a time constant of 40 ns (k_{tt} = 2.5 × 10^7 s^{-1}). If one monitors the solution of **2** at 450 nm, where the porphyrin triplet state absorbs strongly, a transient decay is observed whose lifetime is identical with that of the growth of the carotenoid triplet (Figure 4). This result demonstrates clearly that the porphyrin triplet state is indeed the precursor of the carotenoid triplet.

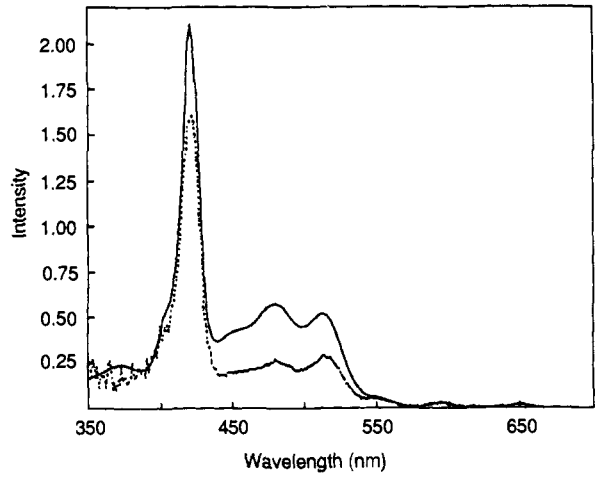

Figure 5. Absorption spectrum (—) and corrected fluorescence excitation spectrum (λ_{em} = 656 nm) (- - -) of carotenoporphyrin **5** in toluene solution. The spectra were normalized in the 585–595 nm region. The singlet–singlet energy transfer efficiency is 0.47.

Similar transient absorption experiments with **1**, **2**, and **3** were carried out in a 2-methyltetrahydrofuran glass at 77 K. Porphyrin-to-carotenoid triplet–triplet energy transfer was again observed, and the rise times of the carotenoid triplet absorptions at 550 nm were identical with those found at ambient temperatures.

Singlet–Singlet Energy Transfer. Carotenoid-to-porphyrin singlet–singlet energy transfer is conveniently studied using steady-state fluorescence excitation spectroscopy. As an example, consider carotenoporphyrin **5**, in which the carotenoid is joined to the porphyrin through the ortho position of an aromatic ring with an amide linkage which is reversed, compared to those in **1–3**. Excitation of a toluene solution of **5** in the Soret band at 422 nm yields a typical corrected free base porphyrin emission spectrum with two maxima at 656 and 722 nm.

If the porphyrin fluorescence is monitored at 656 nm and the excitation spectrum is measured, the results shown in Figure 5 are obtained. In the figure, the corrected excitation spectrum has been multiplied by a factor in order to normalize it to the absorption spectrum of **5** in the 585–595 nm region where the carotene moiety does not absorb appreciably. It is clear that, in

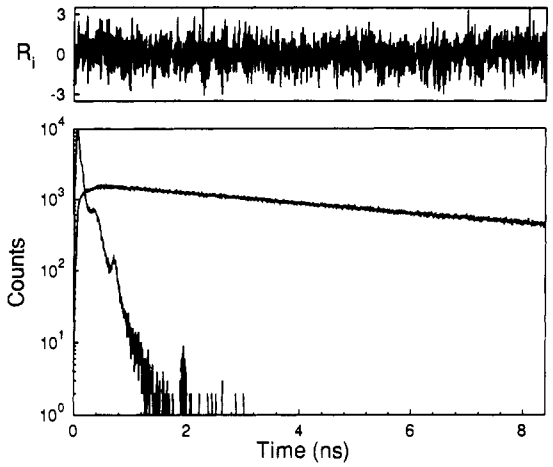

Figure 6. Decay of the porphyrin fluorescence at 720 nm of a 1×10^{-5} M solution of para-linked carotenoporphyrin **1** following excitation at 590 nm. The experimental data, instrument response function, best fit to the data using a single exponential function, and residuals (R_i) are shown. The fluorescence lifetime is 5.2 ns ($\chi^2 = 1.07$).

regions where the carotenoid *does* absorb, carotenoid features are apparent in the spectrum. Thus, singlet–singlet energy transfer from the carotenoid to the porphyrin is occurring.

$$C\text{–}P \xrightarrow{h\nu} {}^1C\text{–}P \tag{4}$$

$$^1C\text{–}P \xrightarrow{k_{et}} C\text{–}{}^1P \tag{5}$$

However, the fact that the excitation and absorption spectra are not coincident in these regions shows that the transfer is not complete. Quantitatively, the singlet–singlet energy transfer efficiency is ~47%, as estimated from the ratio of the normalized corrected excitation spectrum to the absorption spectrum at the carotenoid maxima in the 450–525 nm region. Similar experiments were carried out for carotenoporphyrins **1**, **2**, **3**, and **4**. The transfer efficiencies were found to be 13%, 10%, 17%, and 20%, respectively.

Porphyrin Fluorescence Quenching. As mentioned above, carotenoids have been observed to quench the first excited singlet states of nearby porphyrins. This phenomenon was investigated in carotenoporphyrins **1–3** using the time-correlated single photon counting technique (see the Experimental Section). The time response of the apparatus was ca. 35 ps. The compounds were dissolved in toluene (ca. 1×10^{-5} M) and deoxygenated with argon, and the decay of porphyrin fluorescence at 650 and 720 nm was measured at ambient temperature with 590-nm excitation. Typical results for **1** are shown in Figure 6. The porphyrin singlet state decays as a single exponential with a lifetime (τ_f) of 5.2 ns ($\chi^2 = 1.07$). The lifetime of model porphyrin **6**, determined under the same conditions, was 11.0 ns ($\chi^2 = 1.13$). Thus, the porphyrin first excited singlet state is indeed quenched by the attached carotenoid. Similar experiments with meta isomer **2** and ortho isomer **3** yielded single exponential decays with lifetimes of 7.2 ns ($\chi^2 = 0.96$) and 5.9 ns ($\chi^2 = 1.10$), respectively.

The rate constants for the additional photochemical process leading to porphyrin fluorescence quenching ($k_{add.}$) may be estimated from eq 6

$$k_{add.} = \frac{1}{\tau_f} - \frac{1}{\tau_f^R} \tag{6}$$

where τ_f^R is the lifetime of the excited singlet state of a model porphyrin which lacks the additional process. Using the 11.0-ns fluorescence lifetime of **6** as a reference, $k_{add.}$ values of 1.0×10^8, 4.8×10^7, and 7.9×10^7 s^{-1} were calculated for **1**, **2**, and **3**, respectively.

The quenching of the porphyrin singlet state by the attached carotenoid is solvent dependent. In deoxygenated acetonitrile, the lifetimes for **1**, **2**, and **3** were 3.9 ($\chi^2 = 1.25$), 5.8 ($\chi^2 = 1.09$), and 1.0 ns ($\chi^2 = 1.07$), respectively, measured at 720 nm. Carotenoporphyrins **1** and **2** gave good fits to single exponentials. Ortho isomer **3** required three exponential components, but the 1.0-ns decay contributed over 80% of the total initial amplitude. The lifetime of model porphyrin **6**, on the other hand, remained at 11.0 ns in deoxygenated acetonitrile (one exponential with $\chi^2 = 1.22$).

The fluorescence quantum yields for **1–3** were determined in deoxygenated toluene solutions by comparing the corrected integrated fluorescence intensities using tetraphenylporphyrin ($\phi_f = 0.11$)[32] as a standard. Excitation was at 420 nm. The quantum yields were 0.053, 0.079, and 0.055 for **1**, **2**, and **3**, respectively.

The reduced lifetime of the porphyrin first excited singlet state in **1–3** could be due in principle to an increase in the radiative rate constant of the porphyrin, an increase in intersystem crossing to the triplet, or enhanced nonradiative return to the ground state by some mechanism (hereafter referred to as "enhanced internal conversion"). Each of these possibilities will be considered in turn.

Because the absorption spectrum of the porphyrin moiety is not appreciably perturbed by the carotenoid, it seems unlikely that the radiative rate constant for the porphyrin first excited singlet state has changed. If this is indeed the case, the fluorescence quantum yields of **1–3** can be determined from

$$\phi_f^{CP} = \frac{\tau_f^{CP}}{\tau_f^R}\phi_f^R \tag{7}$$

where ϕ_f^{CP} and ϕ_f^R are the fluorescence quantum yields of the carotenoporphyrin in question and a suitable reference porphyrin, and τ_f^{CP} and τ_f^R are the corresponding excited singlet state lifetimes. If one assumes that τ_f^R is 11.0 ns, as was found for **6**, and that ϕ_f^R is 0.11, as has been found for *meso*-tetraphenylporphyrin in cyclohexane solution,[32] then ϕ_f^{CP} would equal 0.052, 0.072, and 0.059 for **1**, **2**, and **3**, respectively in toluene. These numbers are in accord with those found by steady-state fluorescence spectroscopy as reported above. Thus, the radiative rate constant, $k_{rad.}$, for the porphyrin first excited singlet state in the carotenoporphyrins is virtually unchanged from that of the model porphyrin **6** and equals 1.0×10^7 s^{-1}.

This being the case, one can determine whether the quenching of the porphyrin first excited singlet state by the carotenoid is enhanced internal conversion or enhanced intersystem crossing. Given that

$$k_f = k_{rad.} + k_{isc} + k_{ic} + k_{add.} \tag{8}$$

and assuming that the additional pathway is enhanced internal conversion, then the calculated intersystem crossing quantum yield, ϕ'_{isc}, would be

$$\phi'_{isc} = \frac{k_{isc}}{k_{rad.} + k_{isc} + k_{ic} + k_{add.}} \tag{9}$$

where k_f is the reciprocal of the excited singlet state lifetime of the porphyrin, and $k_{rad.}$, k_{ic}, and k_{isc} are the radiative, internal conversion, and intersystem crossing rate constants in the carotenoporphyrin in the absence of any additional decay process. If one assumes that the sums of $k_{rad.}$, k_{ic}, and k_{isc} for carotenoporphyrins **1–3** and model porphyrin **6** are identical, then it can be shown that the ratio of the quantum yield of intersystem crossing for the ortho isomer **3** to that of the meta isomer **2** should be

$$\frac{\phi'^{o}_{isc}}{\phi'^{m}_{isc}} = \frac{k_6 + k_{add.}^{m}}{k_6 + k_{add.}^{o}} \tag{10}$$

where k_6 is the reciprocal of the 11.0-ns lifetime of the excited singlet state of **6**. This ratio is calculated to be 0.82:1. The corresponding calculation was performed for the para isomer **1** to give intersystem crossing quantum yield ratios of 0.73:1:0.82 for **1**:**2**:**3**, respectively.

Alternatively, if one assumes that the additional decay process is enhanced intersystem crossing, then a related set of calculations

(32) Kikuchi, K.; Kurabayashi, Y.; Kokubun, H.; Kaizu, Y.; Kobayashi, H. *J. Photochem. Photobiol. A* **1988**, *45*, 261.

Table I. ^{1}H NMR Chemical Shifts and $\Delta\delta^a$ Values for Carotenoporphyrins and a Model Carotenoid (in ppm)

		1		2		3	
proton[b]	7 δ	δ	$\Delta\delta$	δ	$\Delta\delta$	δ	$\Delta\delta$
C1′,5′	7.53	7.62	0.09	7.44	−0.09	6.47	−1.06
C2′,4′	7.83	8.00	0.17	7.83	0.00	6.42	−1.41
C8′[c]	7.00	7.07	0.07	6.92	−0.08	6.32	−0.68
C7′[c]	6.60	6.67	0.07	6.52	−0.08	5.96	−0.64
C19′	2.06	2.10	0.04	2.01	−0.05	1.70	−0.36

[a] $\Delta\delta = \delta_{CP} - \delta_7$. [b] See Figure 7 for numbering system. [c] These assignments for 7 are reversed from those in previous reports.[13,22,38]

yields intersystem crossing quantum yield ratios of 1.04:1.00:1.07 for **1**:**2**:**3**, respectively (assuming that k_{isc} is 6.1×10^7 s^{-1}, based on $\phi_{isc} = 0.67$ for **6**[33,34]). As mentioned above, the experimentally determined ratio was 0.74:1.00:0.84. Thus, the experimental ratio is in good agreement with the conclusion that the additional pathway for decay of the porphyrin first excited singlet state is enhanced internal conversion in some form.

Molecular Conformations. In order to interpret the photochemical results presented above in terms of molecular structure, information concerning the conformations of the carotenoporphyrins is needed. The porphyrin and carotenoid moieties are expected to be relatively rigid structures. Although the partial double bond character of the trans amide linkage imparts a certain rigidity and prevents large-scale folding of the molecule about this bond, some of the other bonds in the linker joining the porphyrin and carotenoid moieties are single, and the conformation about these bonds cannot be predicted with confidence from a simple examination of molecular models. Two approaches to the conformational analysis of **1**, **2**, and **3** yielded helpful information: ^{1}H NMR spectroscopy and molecular mechanics calculations.

^{1}H NMR Spectroscopic Studies. ^{1}H NMR spectroscopy can provide fairly precise structural data for the carotenoporphyrins. Immersion of the porphyrin ring system in a strong magnetic field gives rise to large aromatic ring currents, which may be thought of as a circulation of π-electrons in a plane parallel to that of the porphyrin ring. The circulating electrons produce a local magnetic field that opposes the external field. Thus, a proton in the region of the porphyrin ring will experience the sum of the external and other fields *and* the local ring current field and will have its resonance position shifted accordingly. These shifts can be quite large (up to several ppm). The porphyrin ring current induced shift for a carotenoid proton is therefore a sensitive function of the spatial relationship of that proton to the porphyrin macrocycle.

Several theoretical and experimental approaches to the quantitative evaluation of the porphyrin ring current have appeared.[35-37] In this and previous work,[13,22,38] we have adapted the ring current model of Abraham and co-workers[36,37] for the computer-assisted conformational analysis of carotenoporphyrins. The first step in such an analysis is the determination of the ring current induced resonance shifts ($\Delta\delta$) for carotenoid protons from the spectral assignments of the carotenoporphyrins and model compounds. The porphyrin ring current model is then used to determine the molecular conformations consistent with these shifts.

The ^{1}H NMR spectra of **1**–**3** were determined in deuteriochloroform at 300 or 500 MHz, and the resonances were assigned by comparisons with model compounds, single-frequency proton decoupling experiments, and various modifications of the COSY homonuclear shift-correlated 2-D experiment. The numbering

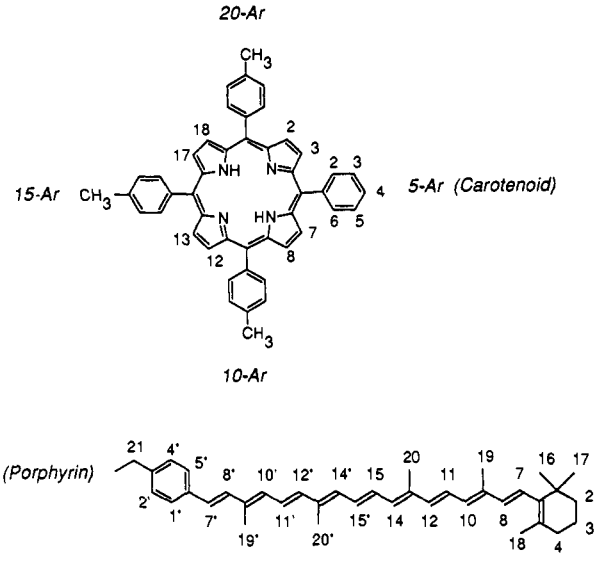

Figure 7. Numbering system for NMR analysis of carotenoporphyrins. In the tables, the carotenoid resonance numbers are preceded by the letter C.

system used to identify the protons on the various molecular fragments is shown in Figure 7. It was found that the only carotenoid protons whose resonances were significantly shifted by the attached porphyrin were those on the aryl ring (C1′,5′ and C2′,4′), the first double bond in the polyene chain (C7′ and C8′), and the methyl group (C19′). The chemical shift values for these protons in **1**–**3** are listed in Table I.

Calculation of $\Delta\delta$ requires the use of a model compound, which ideally should include all structural features present in the carotenoporphyrin itself except for the porphyrin ring current. Previous work[22] has shown that carotenoid aniline amide **7** is a good model for compounds of this type. The relevant chemical shifts for **7** are given in Table I, as are the $\Delta\delta$ values, calculated as $\delta_{CP} - \delta_7$. Thus, negative $\Delta\delta$ values signify an upfield shift (shielding).

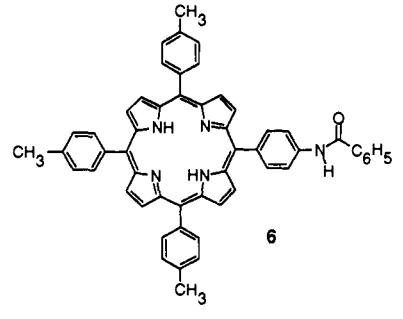

6

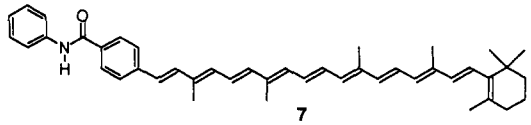

7

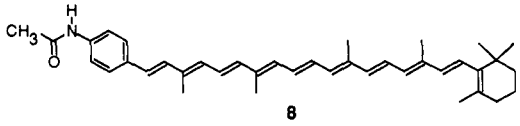

8

The method used for the calculation of molecular conformations from the ring current induced shifts was the single-equivalent-dipole model of Abraham et al. and has been discussed previously.[22] The calculation takes account of the small effects of the ring currents of the three meso aromatic rings of the porphyrin moiety which do not bear the carotenoid (the effect of the fourth ring is included in the model compound chosen). The calculations require a knowledge of the orientation of these rings with respect to the porphyrin plane. These rings are not coplanar with the

(33) Moore, T. A.; Benin, D.; Tom, R. *J. Am. Chem. Soc.* **1982**, *104*, 7356.
(34) Schmidt, J. A.; McIntosh, A. R.; Weedon, A. C.; Bolton, J. R.; Connolly, J. S.; Hurley, J. K.; Wasielewski, M. R. *J. Am. Chem. Soc.* **1988**, *110*, 1733.
(35) Schulman, R. G.; Wuthrich, K.; Yamane, T.; Patel, D. J.; Blumberg, W. E. *J. Mol. Biol.* **1970**, *53*, 143.
(36) Abraham, R. J.; Fell, S. C. M.; Smith, K. M. *Org. Magn. Reson.* **1977**, *9*, 367.
(37) Abraham, R. J.; Bedford, G. R.; McNeillie, D.; Wright, B. *Org. Magn. Reson.* **1980**, *14*, 418.
(38) Chachaty, C.; Gust, D.; Moore, T. A.; Nemeth, G. A.; Liddell, P. A.; Moore, A. L. *Org. Magn. Reson.* **1984**, *22*, 39.

Table II. Carotenoporphyrin Conformations from NMR Chemical Shifts

compd	ϕ_1	ϕ_2	ϕ_4	ϕ_5	$\Delta\Delta\delta^a$	$R_{ee}{}^b$	$R_{cc}{}^c$	κ_1^2	κ_{11}^2
				Para Isomer					
1a	45	45	180	0	0.004[d]	7.9	24.7	1.75	1.82
1b	45	45	180	180		7.9	24.1	1.70	1.73
1c	45	135	180	0		7.9	24.7	1.26	2.38
1d	45	135	180	180		7.9	24.1	0.83	1.75
				Meta Isomer					
2a	70	10	45	0	0.036[d]	6.5	22.5	2.09	0.44
2b	70	10	45	180		6.5	21.1	0.76	0.49
				Ortho Isomer					
3a	65	45	30	0	0.03[d]	4.0	16.4	0.65	0.63
3b	65	45	30	180		4.0	16.1	0.07	0.01

[a] Average difference between observed and calculated $\Delta\delta$ values (in ppm) for the protons listed in Table I. [b] Edge-to-edge distance in angstroms (see text). [c] Center-to-center distance in angstroms (see text). [d] This is the $\Delta\Delta\delta$ value assuming rapid interconversion on the NMR time scale of the listed isomers.

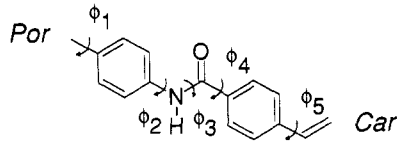

Figure 8. Dihedral angles defining the relative relationship of the porphyrin and carotenoid moieties.

macrocycle for steric reasons. As discussed previously,[22,38] we have assumed that these rings reside in two equally populated conformations at angles of 45° with respect to the plane of the macrocycle.

The conformational analysis of the carotenoporphyrins may be simplified by considering only torsions about the single bonds in the linkage joining the porphyrin and carotenoid moieties, as the force constants for other intramolecular motions which could significantly affect conformation are doubtless much larger. The bond lengths, bond angles, and other dihedral angles are fixed at those values found for model compounds by X-ray diffraction studies. The numbering system used to identify the important dihedral angles is shown in Figure 8. The convention used for assigning dihedral angles is that they are measured clockwise when looking down the linkage bond from the end closest to the porphyrin macrocycle. The 0° conformation is that in which the bonds of the main linkage chain are eclipsed.

The conformational analysis for each carotenoporphyrin consisted of choosing an arbitrary starting conformation, calculating a $\Delta\delta$ value for each of the protons in Table III on the basis of the appropriate distances and angles for that conformation, determining the differences between the observed and calculated $\Delta\delta$ values, and then changing the dihedral angles ϕ_1, ϕ_2, ϕ_4, and ϕ_5 as necessary and recalculating in order to minimize these differences. We have reported a computer program which automatically carries out this procedure.[38]

Table II shows the conformations of **1**, **2**, and **3** which gave the best fits to the experimental data, along with the average difference between the measured and calculated $\Delta\delta$ values for the protons listed in Table I. Representative conformations for **1**–**3** are shown pictorially in Figures 9–11.

As shown in Figure 9, para isomer **1** adopts an extended conformation in which the carotenoid is directed out, away from the porphyrin. This general arrangement is forced on the molecule by the amide bond in the linkage. Although only one conformation for **1** is illustrated, there are actually four different but closely related conformers which would be expected to be of essentially equal energy and therefore equally populated (Table II). Two conformations differing by 90° at ϕ_2 are expected, as are two conformations differing by 180° at ϕ_5. These will interconvert at a rate which is rapid on the NMR time scale. Averaging the proton chemical shifts for these four conformations yields an average difference between the measured and calculated $\Delta\delta$ values of only 0.004, which is well within the accuracy of measurement.

The magnitude of ϕ_1 for the para isomer is not directly assessed by the ^{1}H NMR results described above. As mentioned, previous NMR work is most consistent with a value of ca. ±45°. However, the NMR studies of the closely related **2** and molecular mechanics calculations yield values of 65°–70° (see below), which are in accord with X-ray studies of crystalline porphyrins.[39,40] Thus, the 45° value may be somewhat too low. In that case, a compensating adjustment of ϕ_2 would give a conformation of the carotenoid polyene, relative to the porphyrin, which is identical to that in Table II.

The $\Delta\delta$ values for meta isomer **2** (Table I) are all relatively small and mostly negative. This indicates that the carotenoid aryl ring and the first double bond in the unsaturated chain are slightly into the shielding region above the porphyrin plane. Thus, although analogy with **1** might suggest that there would be four likely conformations about ϕ_2, only one of these, with ϕ_2 equal to 45°, allows the carotenoid to enter the shielding region, and this occurs only when angle ϕ_1 is increased to ≥65°. The best fit is achieved for the conformation indicated in Figure 10 and Table II, with Φ_1 equal to 70°. As is the case for **1**, Φ_5 is allowed to take values of either 0° or 180°, and the molecule is assumed to rapidly interconvert between these two conformations on the NMR time scale.

The large, negative $\Delta\delta$ values for ortho isomer **3** (Table I) show that in this molecule the carotenoid lies far into the shielding region above the porphyrin macrocycle. Thus, the carotenoid is folded across the porphyrin. The quantitative analysis gave the best fit to the data for the conformation shown in Figure 11 and Table II, with again a rapid interconversion between nearly isoenergetic conformers with Φ_5 equal to 0° and 180°.

Molecular Mechanics Calculations. There are some potential ambiguities associated with the NMR method of conformational analysis. The NMR time scale for chemical exchange is very slow compared to the usual rates of rotation about single bonds. As a result, the NMR chemical shifts determined above may represent time averages of several populated conformations. These can be logical groups of related conformers as discussed above, but they need not be. A consequence of this fact is that sparsely populated conformations might in principle be sampled by a large fraction of the molecules on the time scale of a particular photochemical process, but would be undetected by the NMR experiment. In addition, the validity of the NMR analysis is limited by the limitations of the ring current model and by the assumption that the observed $\Delta\delta$ values are due only to the ring currents. These problems are not expected to be of major importance for the purposes of this study because the gross features of the linkage constrain the likely conformations to a relatively small region of space. Nevertheless, it was felt that a conformational analysis using molecular mechanics methods would be a valuable complement to the NMR study.

The molecular mechanics calculations were performed using the CHARMm program in the QUANTA molecular modeling package from Polygen Corporation. The calculations involved

(39) Hoard, J. L. *Science* **1971**, *174*, 1295.
(40) Hoard, J. L. *Porphyrins and Metalloporphyrins*; Smith, K. M., Ed.; Elsevier: New York, 1975; p 317.

Table III. Carotenoporphyrin Conformations from Molecular Mechanics

compd	ϕ_1	ϕ_2	ϕ_4	ϕ_5	R_{ee}[a]	R_{cc}[b]	κ_1^2	κ_{11}^2
				Para Isomer				
1e	60	358	51	180	8.0	25.1	1.96	3.31
1f	60	0	49	0	8.0	23.9	1.74	1.57
1g	60	358	130	182	8.0	23.9	1.47	1.92
1h	60	359	129	0	8.0	25.1	2.13	1.61
				Meta Isomer				
2c	61	183	132	1	7.1	23.0	1.85	0.58
2d	60	182	133	182	7.1	19.7	0.11	1.71
				Ortho Isomer				
3c	62	186	159	11	4.6	17.8	0.13	0.45
3d	60	188	156	186	4.7	14.1	0.01	1.20

[a] Edge-to-edge distance in angstroms (see text). [b] Center-to-center distance in angstroms (see text).

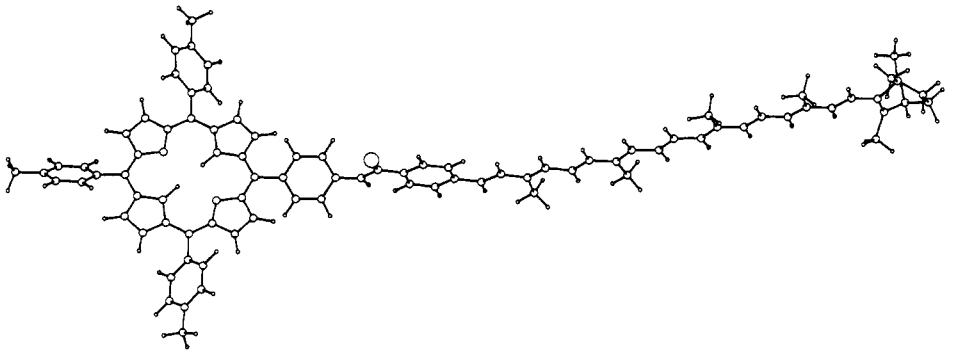

Figure 9. Conformation of para isomer **1** as deduced from ^{1}H NMR chemical shifts.

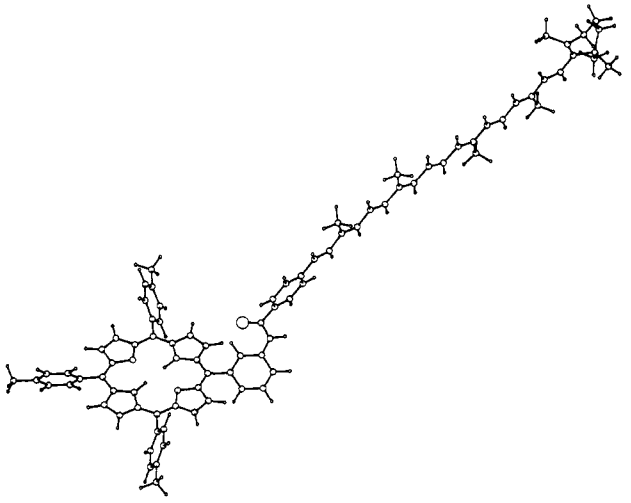

Figure 10. Conformation of meta isomer **2** as deduced from ^{1}H NMR chemical shifts.

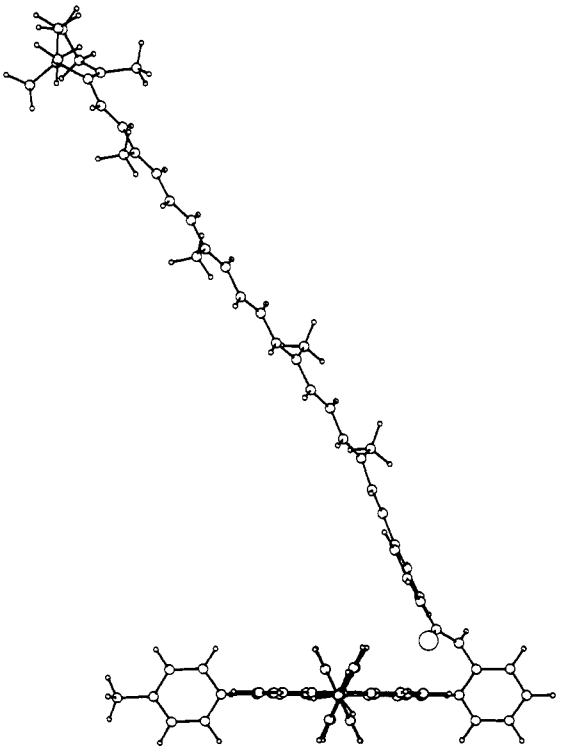

Figure 11. Conformation of ortho isomer **3** as deduced from ^{1}H NMR chemical shifts.

defining the force field for the carotenoporphyrins, followed by energy minimization. The force field is assigned by the choice of suitable atom-type parameters, which combine to define the force constants for the various bonds and other interactions. For most of the atoms of the carotenoporphyrins, the usual CHARMm atom types were retained. However, it was necessary to increase the force constants for torsion about the bonds in the porphyrin macrocycle itself in order to force the program to minimize to a porphyrin structure similar to those observed by X-ray crystallography.

The minimization procedure was an adopted basis Newton–Raphson method suitable for relatively large molecules. It still proved necessary to minimize the energies of the porphyrin and carotenoid moieties individually and then to constrain these structures and allow the final minimization to occur only about the bonds in the linker. The results for **1**, **2**, and **3** are presented numerically in Table III and pictorially in Figures 12–14, respectively. As was the case for the conformational analysis by NMR, four essentially equal energy conformers were found for para isomer **1**, whereas the meta and ortho isomers yielded two similar conformations in which the angle ϕ_5 assumed values of approximately 0° and 180°.

Comparison of the results of conformational analysis by NMR and molecular mechanics methods shows that, although the values of the dihedral angles in the linkages differ substantially for the two methods, the gross aspects of the final conformations and interchromophore relationships are strikingly similar. This increases one's confidence in both methods.

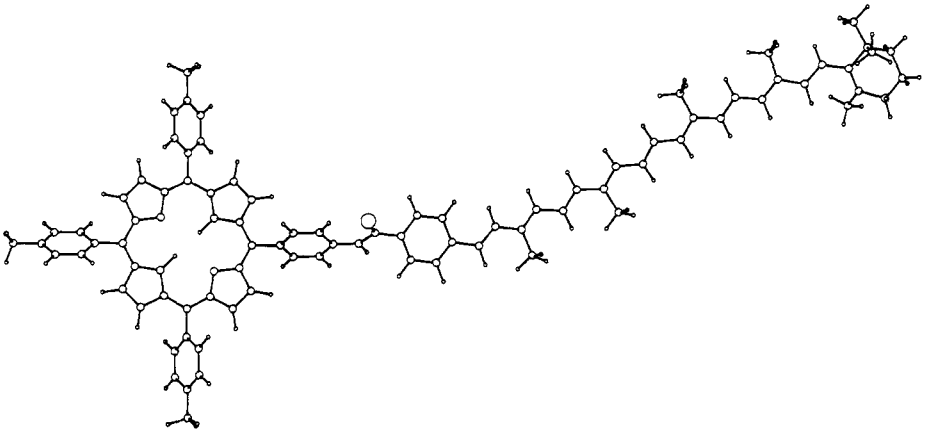

Figure 12. Conformation of para isomer **1** as deduced from molecular mechanics calculations.

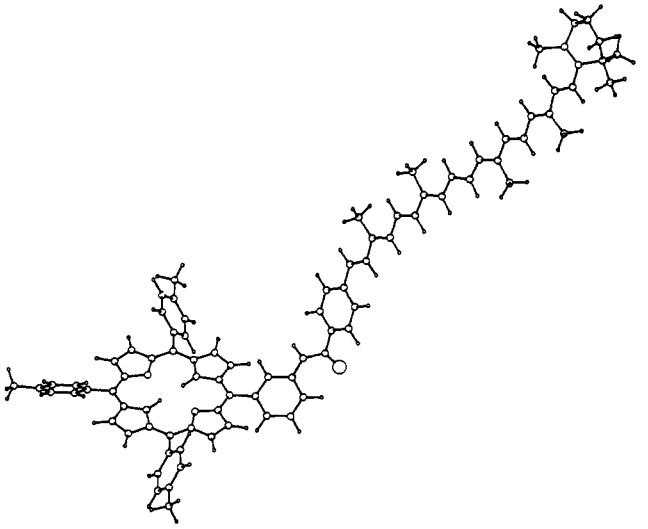

Figure 13. Conformation of meta isomer **2** as deduced from molecular mechanics calculations.

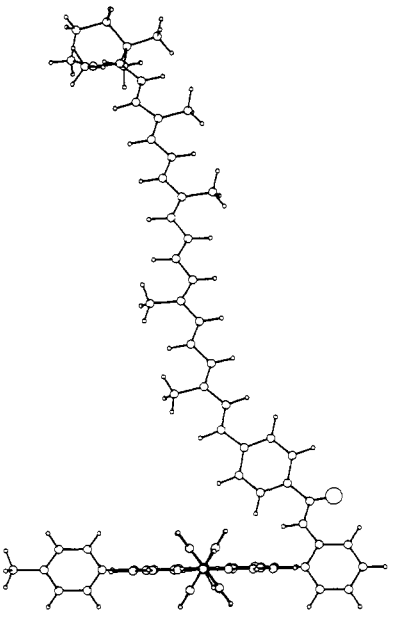

Figure 14. Conformation of ortho isomer **3** as deduced from molecular mechanics calculations.

Discussion

The results of these studies show that there are three photochemical processes occurring in the carotenoporphyrins which involve interchromophoric interactions. One of these is triplet–triplet energy transfer from the porphyrin to the carotenoid, a second is singlet–singlet transfer from the carotenoid to the porphyrin, and the third is an additional pathway for internal conversion in the porphyrin singlet manifold. Figure 15 shows the rate constants for these three processes (or their lower limits) plotted as a function of the position of substitution. It is readily apparent that, although the rates of the three processes are quite different from one another, they all follow the same trend. The rates for the meta isomer **2** are always slower than those for the other two carotenoporphyrins. This interesting observation sheds light on the mechanisms of the three photochemical processes, as discussed below.

Triplet–Triplet Energy Transfer. The quenching of the porphyrin triplet state (with an energy of ca. 1.5 eV) by energy transfer to the attached carotenoid (with a triplet energy below 1.0 eV) is presumed to occur via an electron-exchange mechanism. A simple visualization of this process is a concerted transfer of one electron from the LUMO of the porphyrin to the LUMO of the carotenoid and a second electron from the HOMO of the carotenoid to the HOMO of the porphyrin.[41,42] Such a mechanism requires spatial overlap of the orbitals in question. It is commonly assumed that, at relatively large separations, molecular

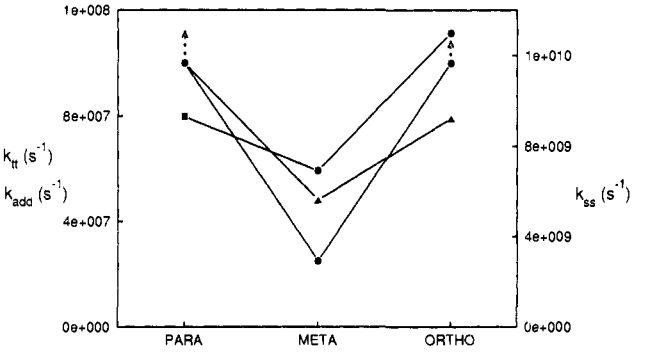

Figure 15. Comparison of the rates of triplet–triplet energy transfer (●), singlet–singlet energy transfer (based on the carotenoid S_1 state) (■), and the additional pathway for decay of the porphyrin first excited singlet state (▲) as a function of structure for the para (**1**), meta (**2**), and ortho (**3**) carotenoporphyrin isomers.

wave functions fall off exponentially with distance. Given this, Dexter[43] has proposed that the rate constant for exchange-mediated triplet–triplet energy transfer is given by

$$k_{tt} = KJ \exp(-2R_{DA}/L) \qquad (11)$$

where K is related to the specific orbital interactions and J is a

(41) Turro, N. J. *Modern Molecular Photochemistry*; Benjamin/Cummings: Menlo Park, CA, 1978; p 307.
(42) Closs, G. L.; Johnson, M. D.; Miller, J. R.; Piotrowiak, P. *J. Am. Chem. Soc.* **1989**, *111*, 3751.
(43) Dexter, D. L. *J. Chem. Phys.* **1953**, *21*, 836.

spectral overlap integral of the donor emission and the acceptor absorption which is normalized for the extinction coefficient of the acceptor. The quantity R_{DA} is the donor–acceptor separation, and L is an "effective average Bohr radius".[43]

A cursory examination of eq 11 shows that in this simple form it cannot possibly explain the trend in triplet–triplet transfer rates shown in Figure 15. This is the case because although K and J would be expected to be identical for isomers **1–3**, to a first approximation, the distance R must decrease in going from para to meta to ortho carotenoporphyrin. Quantitative application of eq 11 requires a knowledge of R for the three molecules. For estimating orbital overlap, it makes sense to choose the distance of closest approach of the edges of the π-electron systems, since neither the donor nor the acceptor electron distributions are spherical. For the purposes of this discussion, we have taken this distance as that between the aryl ring carbon atom of the carotenoid which is attached to the amide linkage (C3′ in Figure 7) and the meso carbon of the porphyrin which bears the carotenoid moiety (P5). This distance is given as R_{ee} in Table II. Now consider the meta isomer **2**, for which k_{tt} is determined to be 2.5×10^7 s^{-1}. Using this value, an R of 6.5 Å, and an L of 1.5 Å (which has been found to be appropriate for two interacting aromatic systems),[44,45] the quantity KJ may be calculated to be 1.5×10^{11} s^{-1}. Using this KJ value, rates of 4.0×10^6 s^{-1} and 7.2×10^8 s^{-1} may be calculated for **1** and **3**, respectively. The experimental results given above show that *both* of these rates must be greater than 1×10^8 s^{-1}. Thus, the k_{tt} for para isomer **1** predicted by the simple Dexter treatment is much smaller than the experimental value. The predicted value will of course be different for other choices of L, but the trend will be the same.

Clearly, another explanation must be sought. One could of course make more sophisticated estimates of orbital overlap between the porphyrin donor moiety and the carotenoid acceptor. However, the structures and conformations of the molecules suggest that finding a better "through-space" overlap between these orbitals in the para isomer than in the meta isomer would be very unlikely. It seems more reasonable to propose that the chemical bonds of the amide linker joining the two moieties mediate the energy transfer. Indeed, a variety of examples of "through-bond" triplet energy[42,46,47] and electron[46–48] transfer (which also occurs by a mechanism involving orbital overlap) have been reported. However, such a postulate in its simplest form still does not rationalize the experimental data, because there are fewer covalent bonds on the shortest path joining the chromophores in the meta compound than in the para isomer.

If we postulate that the energy transfer takes place mainly via the π-bonds of the linkage, however, the trends in Figure 15 can be readily explained, as the electronic coupling of the chromophores via the para and ortho linkages should be stronger than that through the meta linker. To illustrate this conclusion, it is convenient to consider the through-bond transfer as a case of superexchange coupling. The superexchange coupling, V_{se}, between a donor state d and an acceptor state a via a linker state l is given by

$$V_{se} = \frac{V_{dl}V_{la}}{\Delta E_{dl}} \tag{12}$$

where V_{dl} and V_{la} are the electronic coupling between states d and l, and l and a, respectively, and ΔE_{dl} is the energy difference between states d and l.[49,50] In this mechanism, the linker state l is never actually populated during the transfer, but simply increases the electronic coupling between the donor and acceptor states by mixing with them. In terms of the pictorial electron-exchange description for triplet–triplet energy transfer discussed above, the process could be envisaged at the simplest level as transfer of an electron from the LUMO of the porphyrin donor to the LUMO of the carotenoid acceptor, which is facilitated by the LUMOs of the linker, and a concurrent transfer in the other direction involving the HOMOs of the donor, linker, and acceptor.

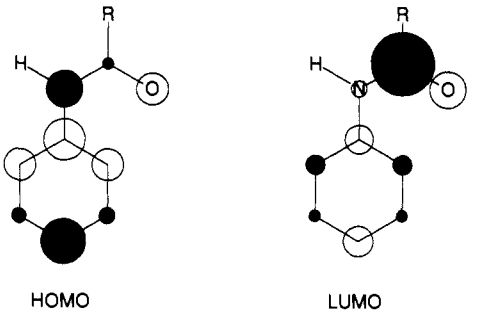

Figure 16. Results of Hückel molecular orbital calculations for the linkage joining the carotenoid and porphyrin moieties of **1–3**.

Qualitatively, this superexchange, or through-bond, proposal was evaluated using Hückel molecular orbital theory at the most basic level.[51] The linker was considered to consist of the meso aryl ring at P5 and the attached amide group. If one considers the partial double bond nature of the amide, then the porphyrin π-electron system and that of the carotenoid are formally conjugated through the linker. In practice, this conjugation is partially interrupted by the twisting of the meso aryl ring out of plane with the porphyrin and by any deviations from planarity at each end of the amide group. Thus, the two chromophores retain their individuality, as demonstrated by the fact that the inherent photophysical properties of the two chromophores are little affected by linking them. Superexchange interactions between these chromophores could then occur via the HOMO and LUMO of the linker; these orbitals are the ones examined using the Hückel treatment.

The calculation is straightforward, except for the fact that two of the atoms involved in the conjugated system are non-carbon. Thus, the values of the empirical α and β parameters for these atoms, X (associated with the coulomb and resonance integrals, respectively), differ from the standard values. The usual method for treating this problem is via eqs 13 and 14, where α_0 and β_0 are the standard values for carbon.

$$\alpha_X = \alpha_0 + h_X\beta_0 \tag{13}$$

$$\beta_{CX} = K_{CX}\beta_0 \tag{14}$$

Values of 1.0 and 1.5 for h_O and h_N, respectively, were chosen, with k_{CX} equal to 1.0 in each case.[51,52] The h value chosen for nitrogen is usually deemed appropriate for a nitrogen which contributes both of its formally unshared electrons to the π-system. However, changing h_N to 0.5 (as suggested for pyridine-type nitrogen atoms) yields the same trends.

The results of the calculation are shown in Figure 16. The radius of the circle at each atom is proportional to the coefficient of the wave function at that atom, the area is proportional to the orbital density, and the shading is proportional to the relative sign of the wave function at that point. The carotenoid polyene will be attached at the position of the R group in each of the carotenoporphyrins **1–3**. However, the position of the porphyrin will vary. Thus, it is of interest to examine the relative orbital densities at the aryl positions ortho, meta, and para to the nitrogen. It is

(44) Oevering, H.; Verhoeven, J. W.; Paddon-Row, M. N.; Cotsaris, E.; Hush, N. S. *Chem. Phys. Lett.* **1988**, *143*, 488.
(45) Inokuti, M.; Hirayama, F. *J. Chem. Phys.* **1965**, *43*, 1978.
(46) Closs, G. L.; Piotrowiak, P.; MacInnis, J. M.; Fleming, G. R. *J. Am. Chem. Soc.* **1988**, *110*, 2652. Sigman, M. E.; Closs, G. L. *J. Phys. Chem.* **1991**, *95*, 5012.
(47) Closs, G. L.; Miller, J. R. *Science* **1988**, *240*, 440.
(48) Oevering, H.; Paddon-Row, M. N.; Heppener, M.; Oliver, A. M.; Cotsaris, E.; Verhoeven, J. W.; Hush, N. S. *J. Am. Chem. Soc.* **1987**, *109*, 3258. Verhoeven, J. W.; Paddon-Row, M. N.; Hush, N. S.; Oevering, H.; Heppener, M. *Pure Appl. Chem.* **1986**, *58*, 1285. Warman, J. M.; de Haas, M. P.; Paddon-Row, M. N.; Cotsaris, E.; Hush, N. S.; Oevering, H.; Verhoeven, J. W. *Nature (London)* **1986**, *320*, 615.
(49) Kramers, H. A. *Physica* **1934**, *1*, 182.
(50) Bixon, M.; Jortner, J.; Michel-Beyerle, M. E.; Ogrodnik, A. *Biochim. Biophys. Acta* **1989**, *977*, 273.
(51) Greenwood, H. H. *Computing Methods in Quantum Organic Chemistry*; Wiley-Interscience: London, 1972.
(52) Streitwieser, A. J. *Molecular Orbital Theory for Organic Chemists*; John Wiley and Sons: New York, 1961; pp 120–135.

clear that, for both the HOMO and the LUMO, the orbital density is greater at the ortho and para positions than it is at the meta positions. This being the case, it seems reasonable to suggest that the electronic coupling of the carotenoid and the porphyrin, as mediated by the superexchange interaction, will also be greater at the ortho and para positions. This provides a simple rationalization of the triplet–triplet electron-transfer trends noted in Figure 15.[53]

Additional support for the involvement of the π-electrons of the linker bonds in the triplet–triplet energy transfer comes from results previously reported for carotenoporphyrins **9–11**.[22] In these molecules, the carotenoid is joined to the porphyrin at the ortho, meta, or para position of a meso aryl ring via CH_2O linkages. In a polystyrene glass the rates of triplet–triplet energy transfer were 2.2×10^6, 3.1×10^6, and 4.4×10^6 s^{-1} for **9–11**, respectively. ^1H

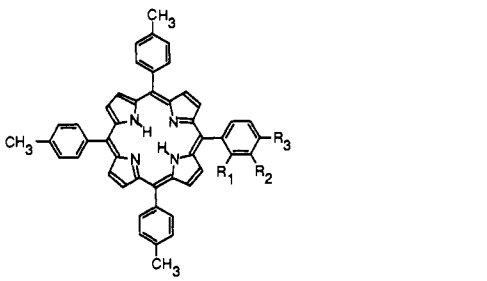

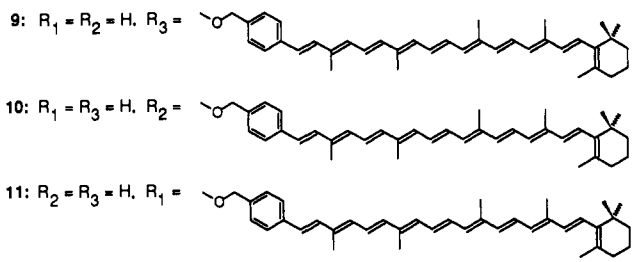

NMR studies showed that the conformations of these molecules varied from extended (for **9**) to folded (for **11**) in a way reminiscent of **1–3**. Two interesting comparisons between the results for **1–3** and those for **9–11** can be made. In the first place, k_{tt} is considerably faster for the amide-linked molecules than for those with the ether linkage, even though the number of bonds joining the two aryl rings is identical. In the case of the ortho and para molecules, this difference may be 100-fold or greater. This result is consistent with enhanced through-bond triplet–triplet energy transfer due to the availability of the conjugated π-electrons in the amide bridge in **1–3**, but not in **9–11**. Secondly, the rates for **9–11** increase on going from para to meta to ortho linkages, as would be expected for through-space transfer or transfer mediated by the single bonds of the linker. This, of course, was not observed for the amide series of molecules.

In benzene solution at ambient temperatures, k_{tt} was found to be 3.6×10^6, 2.2×10^7, and 1×10^8 s^{-1} for **9**, **10**, and **11**, respectively. Under these conditions, internal rotations about the linker bonds are facile, and these motions control triplet energy transfer for the meta and ortho molecules by bringing the chromophores close together and enhancing the through-space coupling. As mentioned above, k_{tt} for **2** does not change when the molecule is frozen in a glass at 77 K. This suggests that in the amide series **1–3**, in which the linker is more rigid and the through-bond interactions stronger, the transfer is completely controlled by through-bond interactions and that large-scale intramolecular motions are unimportant.

Enhanced Internal Conversion. It is apparent that the rate constant for the additional decay pathway which enhances internal conversion in the carotenoporphyrins, k_{add}, varies with the linkage in the same way as that for triplet–triplet energy transfer (Figure 15). Thus, it is reasonable to suppose that this process also depends in some way on the electronic coupling between the two chromophores. With this possibility in mind, we will examine some possible explanations for the enhanced internal conversion.

An early observation of the *inter*molecular quenching of chlorophyll fluorescence by carotenoids was interpreted in terms of electron transfer from the carotenoid to the chlorophyll first excited singlet state.[12] Intramolecular quenching in a number of carotenoporphyrins and related materials has been observed,[13,14] and electron transfer has also been suggested as a possibility (eq 15), although no direct observation of the ions by transient absorption spectroscopy has yet been reported.

$$C\text{-}{}^1P \rightarrow C^{\bullet+}\text{-}P^{\bullet-} \qquad (15)$$

The fact, noted above, that the fluorescence quenching is moderately increased in the more polar acetonitrile solvent is consistent with photoinitiated electron transfer, as such reactions often occur more rapidly in acetonitrile than in toluene. Alternative explanations include singlet–singlet energy transfer from the porphyrin to the carotenoid S_1 state[15] and enhanced internal conversion due to the perturbation of the porphyrin first excited singlet state by the attached carotenoid π-electron system. The energy-transfer explanation would, of course, require that the carotenoid S_1 state lie near or below the porphyrin first excited singlet state in energy.

Electron transfer would have to occur by a mechanism which depends upon overlap of donor and acceptor wave functions, just as is the case for triplet–triplet transfer. In fact, electron transfer in this system may be visualized pictorially in a similar way. An electron is transferred from the HOMO of the carotenoid to the HOMO of the excited porphyrin, with the help of the linker HOMOs via the superexchange mechanism. Thus, the experimental trends are in accord with electron-transfer quenching. However, the trends are also in accord with some other form of enhanced internal conversion, as the mechanism for this would presumably involve some degree of mixing of the porphyrin and carotenoid orbitals. Singlet energy transfer would be consistent with the observations if it, too, occurred by an electron-exchange mechanism.

Singlet–Singlet Energy Transfer. Singlet–singlet energy transfer from the carotenoid to the porphyrin in **1–3** has a dependence on structure similar to that of the other two photophysical processes. With this in mind, it is of interest to investigate the various possible mechanisms for such transfer. In principle, singlet–singlet energy transfer may occur by a trivial emission–absorption mechanism, by the long-range Förster dipole–dipole mechanism or one of its elaborations, or by an electron-exchange mechanism similar to that discussed above for triplet–triplet transfer. A simple calculation rules out the trivial mechanism in this case. As most experimental observations of singlet–singlet transfer are interpreted in terms of the Förster mechanism, we will consider this next.

In its simplest form, Förster transfer is the result of Coulombic interactions between the donor and acceptor transition dipoles. Resonant coupling of the donor "transmitter" and acceptor "receiver" leads to energy transfer. Förster's equation for dipole–dipole energy transfer[54-56] states:

$$k_{ss} = \frac{9(\ln 10)\kappa^2}{128\pi^5 n^4 N' \tau_D^{\circ} R^6} \int f_D(\nu)\, \epsilon_A(\nu)\, \nu^{-4}\, d\nu \qquad (16)$$

In this equation, n is the index of refraction of the solvent, N' is the number of molecules per millimole (Avogadro's constant $\times$ 10^{-3}), τ_D° is the natural fluorescence lifetime of the excited donor (the reciprocal of the radiative rate constant), R is the distance between the centers of the two dipoles in question (in cm), and κ^2 is a function of the relative orientation of the transition dipole moments (see below). The integral (in cm^6/mmol) represents the overlap between the donor emission spectrum and the acceptor

(53) If the angle ϕ_1 is larger for **2** than for **1**, then the loss of conjugation could also contribute to the difference in energy-transfer rates for the two molecules, assuming that a through-bond mechanism involving the π-electrons of the linker is operative.

(54) Förster, T. *Ann. Phys. (Leipzig)* **1948**, *2*, 55.
(55) Förster, T. *Discuss. Faraday Soc.* **1965**, *27*, 7.
(56) Eyring, L. H.; Lin, S. H.; Lin, S. M. *Basic Chemical Kinetics*; John Wiley and Sons: New York, 1980; pp 289–297.

Table IV. Observed and Calculated Singlet–Singlet Energy-Transfer Rate Constants (s^{-1})

	experimental[a]		calcd[b]			
			k_{SS} (S_1)		k_{SS} (S_2)	
compd	k_{SS} (S_1)	k_{SS} (S_2)	κ_1^2	κ_{11}^2	κ_1^2	κ_{11}^2
1	9.3×10^9	6.0×10^{11}				
1a			5.1×10^7	5.3×10^7	3.8×10^{10}	4.0×10^{10}
1b			5.8×10^7	5.9×10^7	4.3×10^{10}	4.4×10^{10}
1c			3.7×10^7	7.0×10^7	2.7×10^{10}	5.2×10^{10}
1d			2.8×10^7	6.0×10^7	2.1×10^{10}	4.4×10^{10}
2	6.9×10^9	4.4×10^{11}				
2a			1.1×10^8	2.3×10^7	7.9×10^{10}	1.7×10^{10}
2b			5.7×10^7	3.7×10^7	4.2×10^{10}	2.7×10^{10}
3	1.3×10^{10}	8.2×10^{11}				
3a			2.2×10^8	2.2×10^8	1.6×10^{11}	1.6×10^{11}
3b			2.7×10^7	3.8×10^6	2.0×10^{10}	2.8×10^9
4	1.6×10^{10}	1.0×10^{12}				
5	5.5×10^{10}	3.6×10^{12}				

[a] These rates were calculated from measured quantum yields based on lifetimes of 16 ps for the carotenoid S_1 state and 250 fs for the S_2 state (see text). [b] These rates were calculated using the Förster equation (eq 16) as discussed in the text. The conformer identification numbers and κ^2 values are taken from Table II.

absorption spectrum, where ϵ_A is the molar decadic extinction coefficient of the acceptor in units of $cm^2/mmol$ (= L/mol·cm) and ν is in cm^{-1}. The value of τ_D° may be calculated from

$$\tau_D = \Phi_f^D \tau_D^\circ \tag{17}$$

where τ_D is the lifetime of the first excited singlet state of the donor in the absence of energy- or electron-transfer processes and Φ_f^D is the corresponding fluorescence quantum yield.

The orientation factor κ^2 depends upon the angle between the transition dipoles and is given by

$$\kappa^2 = (\cos \gamma - 3 \cos \alpha \cos \beta)^2 \tag{18}$$

where α and β are the angles which the transition dipoles make with a line joining the centers of the transitions and γ is the angle between the two transition dipoles.

In the case of the carotenoporphyrins, R will be the distance between the center of the porphyrin macrocycle and the center of the carotenoid π-electron system, taken as the center of the C15–C15′ bond. This distance, R_{cc}, is given in Tables II and III for the various conformations of **1–3**. Calculation of κ^2 requires a knowledge of the transition dipoles of the chromophores. For the porphyrin, the S_1 transition moment will lie along a line joining two opposing pyrrole nitrogen atoms.[57] Thus, for a given carotenoid conformation, there are two possibilities (essentially equally populated), depending upon which nitrogen atoms are protonated. We assume that the transition dipole for the carotenoid lies approximately along the long axis of the carotene, although this may not strictly be the case.[58,59] The two κ^2 values for each conformation of **1–3**, based upon these assumptions, are given in the tables. The index of refraction of toluene is 1.497.[60]

Transfer from the S_1 State of the Carotenoid. Determination of τ_D° and the overlap integral in eq 16 is less straightforward. The S_1 (^2A_g) state of a symmetric carotenoid is formally forbidden and therefore difficult or impossible to observe by absorption or emission spectroscopy. The S_1 state of the carotenoid moiety in **1–5**, in which the symmetry is broken, would be expected to be less forbidden. A recent study of fucoxanthin in ethanol reports a weak emission in the 600–800 nm region, which is attributed to $S_1 \rightarrow S_0$ emission,[61] and other estimates are more or less in agreement with this energy for long polyenes.[62] We have examined the corrected emission spectrum of **7** in toluene and found that, if the $S_1 \rightarrow S_0$ emission does occur in this region (and none was detected), then ϕ_f will be $\leq 1 \times 10^{-5}$ (tetraphenylporphyrin in toluene was used as a standard, with $\phi_f = 0.11$). Picosecond absorption spectroscopy of **8** in toluene shows that the excited state lifetime of the carotenoid is about 16 ps.[29] Using these values for ϕ_f and τ_D, a value of $\geq 1.6 \times 10^{-6}$ s may be calculated for τ_D°. Given the uncertainties noted above, calculation of a reliable overlap integral in eq 16 for the S_1 state of the carotenoid is precluded. We have therefore determined a best case estimate by assuming that all of the donor emission occurred at the 650-nm absorption maximum of the porphyrin. This gives a value of 6.1×10^{-14} cm^6 $mmol^{-1}$ for the overlap integral. Using these values, k_{ss} was calculated for each conformer of **1–3** in Table II. The results are shown in Table IV.

If one assumes that the singlet–singlet energy transfer from the carotenoid is from the S_1 state, then the quantum yield data mentioned above may be used to determine experimental k_{ss} values for **1–5** on the basis of the 16-ps lifetime measured for **8**. These values are also given in Table IV and in Figure 15.

Looking first at the values for the para isomer **1**, it is clear that all eight of the possible conformations for the para molecule give calculated k_{ss} values of about 5×10^7 s^{-1}. The measured values are about 200 times faster. Thus, the simple Förster treatment gives very poor agreement with experiment. This is the case even though the κ^2 values in Table II are substantially larger than the average value of 0.67 for molecules freely tumbling in solution and are approaching the theoretical maximum of 4.0. Turning to the results for the meta isomer **2**, one finds somewhat more variability in the calculated rates, due in large part to the variation in κ^2. However, as mentioned above, for each set of values of ϕ_1–ϕ_5, the two isomers with the differing κ^2 values will be about equally populated. Thus, even in a hypothetical case where only one of the κ^2 values leads to measurable energy transfer, the observed k_{ss} value will be one-half of the value for the isomer with the highest κ^2. Thus, the meta isomers would also be expected to undergo singlet–singlet transfer with a rate of about 5×10^7 s^{-1}. This is because the shorter R_{cc} values for **2** are in part compensated for by the reduced average κ^2. Again, the calculated rates for **2** are more than 100 times slower than the measured rates. Considering finally the ortho isomer **3**, it is apparent that the variation in κ^2 results in substantial variation in calculated rates. Again, one would expect the four isomers in Table IV to be approximately equally populated. In that case, the rate of singlet–singlet energy transfer would be about 1×10^8 s^{-1}. This is again 2 orders of magnitude slower than the observed rate.

To summarize these results, all of the singlet–singlet energy-transfer rates calculated using the Förster dipole–dipole formalism

(57) Gouterman, M. *J. Mol. Spectrosc.* **1961**, *6*, 138.
(58) The transition dipole for the S_2 state is thought to lie approximately along the long axis of the carotenoid π-electron system (see ref 59). In the absence of definitive information, we have assumed that the direction of the S_1 transition dipole was the same.
(59) Shang, Q.-yuan; Dou, X.; Hudson, B. S. *Nature* **1991**, *352*, 703.
(60) Murov, S. L. *Handbook of Photochemistry*; Marcel Dekker: New York, 1973; p 87.
(61) Shreve, A. P.; Trautman, J. K.; Owens, T. G.; Albrecht, A. C. *Chem. Phys.* **1991**, *154*, 171.
(62) Cosgrove, S. A.; Guite, M. A.; Burnell, T. B.; Christensen, R. L. *J. Phys. Chem.* **1990**, *94*, 8118.

are substantially slower than the observed rates. This is true even though the value used for ϕ_f of the carotenoid is an upper limit to the true value and even though the overlap integral is given its maximum possible value, which is without doubt too high. Although a relatively small conformational change in the meta isomer (and a corresponding change in κ^2) might allow one to calculate a rate for the meta isomer which is slower than that observed for the para species, other small changes would give rates considerably faster than those for **1**.

It is possible that the inclusion of higher order (multipole) terms in the Förster description of energy transfer would lead to faster calculated transfer rates. Such an approach seems justified, given the fact that for the carotenoporphyrins the separation of the transition dipoles (R) is comparable to the size of the chromophores. Thus, the dipole–dipole formulation in eq 16 is doubtless an oversimplification. To be helpful, such calculations would not only have to predict substantially higher transfer rates but also have to explain the trends in singlet–singlet energy transfer observed for **1–5**.

Transfer from the S_2 State of the Carotenoid. The problems with rationalizing Förster dipole–dipole singlet energy transfer from the carotenoid S_1 state to porphyrins coupled with recent reports of the photophysics of the carotenoid S_2 state have led investigators to propose that, under some conditions, the S_2 (^1B_u) state might participate in energy transfer.[61,63,64] Emission in the 500–600 nm region has been reported for a number of carotenoids with about the same number of double bonds as **7** and **8**, and this emission has been attributed to $S_2 \rightarrow S_0$.[61,63-65] The lifetime of the S_2 state of β-carotene in ethanol was reported to be 250 fs,[63] and similar lifetimes have been determined for other carotenoids.

Steady-state fluorescence studies of a solution of **7** in toluene resulted in the observation of a broad, weak emission (λ_{max} = 562 nm) in the 500–600 nm region with an excitation spectrum similar to the absorption spectrum of the carotenoid. The quantum yield of emission was ca. 1.6×10^{-4}. This is reasonably close to quantum yields reported for other carotenoids.[61] Assuming that this is indeed carotenoid emission, we can estimate $\tau_D°$ for the S_2 state as 1.6×10^{-9} s, which is in good agreement with the radiative rate constant calculated from the integrated absorption coefficient for the ^1B_u band. From this emission spectrum and the absorption spectrum of **6**, an estimate for the overlap integral of 4.5×10^{-14} cm^6 mmol^{-1} was determined. These values were then used in conjunction with the R_{cc} and κ^2 values in Table II to estimate k_{ss} from the carotenoid S_2 state using eq 16. These results appear in Table IV.

The observed singlet–singlet energy-transfer quantum yields may be converted to transfer rates from the S_2 state on the basis of an estimate of 250 fs for the lifetime of this state. See Table IV for the results.

The Förster calculations based on the S_2 state come considerably closer to rationalizing the experimental results than those for the S_1 state, although the calculated rates for all three isomers are about 1 order of magnitude slower than the observed rates. The observed trends in singlet–singlet transfer rates are not explicitly reproduced by the calculations, but could be by manipulating the κ^2 values.

Conclusions

The results of the triplet–triplet energy-transfer experiments for **1–3** and **9–11** are all in accord with an electron-exchange mechanism in which the π-bonds in the amide linker facilitate the transfer via superexchange interactions which enhance the electronic coupling between the donor and the acceptor.

The trends noted in Figure 15 suggest that a similar mechanism is involved in the quenching of the porphyrin first excited singlet state by the carotenoid. If this additional pathway is electron transfer to form $C^{\bullet+}$–$P^{\bullet-}$, as originally proposed by Beddard and co-workers,[12] then the trend is perfectly understandable, as electron transfer is also mediated by overlap of donor and acceptor wave functions. The through-bond interaction is certainly present, as shown by the triplet–triplet transfer results, and it therefore makes sense to invoke it for the putative electron transfer as well. As mentioned above, other forms of enhanced internal conversion and singlet energy transfer to the carotenoid are also conceivable explanations, and both of these processes could in principle be mediated by through-bond electronic interactions. Transient absorption experiments on the picosecond or subpicosecond time scale will be necessary in order to verify or rule out the electron-transfer mechanism.

Electron transfer from carotenoid ground states to attached porphyrin radical cations does indeed occur and is an important feature of many of the multicomponent photosynthetic reaction center models which have been prepared.[17,30,31] Most of these biomimetic systems feature porphyrin–carotenoid amide linkages identical to those in **1–3**, and the results of the current work suggest that electron transfer from the carotene to the porphyrin radical cation in these molecules is also mediated by the through-bond interaction.

The situation with regard to singlet–singlet energy transfer is less straightforward. It has been previously noted that singlet–singlet transfer from the S_1 state of carotenoids to cyclic tetrapyrroles by a simple dipole–dipole mechanism is very unlikely.[18,27,28,66] On the other hand, there is experimental evidence that, when a carotenoid amine identical to that in **4** and **5** is joined to a pyropheophorbide derivative through an amide linkage, energy transfer occurs only from the S_1 state of the carotenoid to the tetrapyrrole.[29] It is clear from the above discussion that, if a similar process is occurring in **1–5**, the Förster dipole–dipole formalism does not describe the transfer very well. The trends in Figure 15 suggest that the same mechanistic pathway may be operational for both triplet–triplet and singlet–singlet energy transfer. This seems reasonable, as the electron-exchange interaction is clearly present and is strong enough to mediate the triplet–triplet transfer. Why should it not play a role in singlet–singlet transfer as well? Of course, the singlet–singlet transfer occurs much more rapidly than the other photochemical processes, and this might suggest a change in mechanism. On the other hand, the rate of energy or electron transfer depends not only on the spatial details of orbital overlap, which might well be similar for all three processes, but also on energy differences (Franck–Condon terms). In the case of superexchange interactions, this includes not only the energy difference between the initial and final states but also those between the HOMOs and LUMOs of the donor and the linker for each formal electron transfer (eq 12). These energies are quite different for singlet–singlet energy transfer, triplet–triplet transfer, and presumably the putative electron transfer and could account for large differences in rate.

The enhanced singlet–singlet energy transfer quantum yields found for **4** and **5** relative to **1–3** are also consistent with a through-bond electron-exchange mechanism. The spatial relationship of the carotenoid and porphyrin moieties in **1** and **4** in particular would be expected to be very similar, and as a result, the energy-transfer rates via a Förster mechanism should also be very similar. The reversal of the linkage, however, could have a significant effect on the rate of through-bond transfer. INDO and CI calculations of photoinitiated electron-transfer rates through amide linkages indicate significant changes in the electronic coupling of the donor and acceptor through the linkage bonds upon such a reversal.[67]

In this connection, Maruyama and co-workers have recently reported singlet–singlet energy transfer in a series of carotenoporphyrins in which the carotenoid is directly attached to the porphyrin meso ring and therefore conjugated with it.[68] Examination of the data shows that singlet–singlet transfer is faster in

(63) Shreve, A. P.; Trautman, J. K.; Owens, T. G.; Albrecht, A. C. *Chem. Phys. Lett.* **1991**, *178*, 89.
(64) Shreve, A. P.; Trautman, J. K.; Frank, H. A.; Owens, T. G.; Albrecht, A. C. *Biochim. Biophys. Acta* **1991**, *1058*, 280.
(65) Gillbro, T.; Cogdell, R. J. *Chem. Phys. Lett.* **1989**, *158*, 312.
(66) Razi Naqvi, K. *Photochem. Photobiol.* **1980**, *31*, 523.
(67) Scherer, P. O.; Thallinger, W.; Fischer, S. F. *Reaction Centers of Photosynthetic Bacteria*; Michel-Beyerle, M.-E., Ed.; Springer-Verlag: Berlin, 1990; pp 360–362.
(68) Osuka, A.; Yamada, H.; Maruyama, K. *Chem. Lett.* **1990**, 1905.

the para isomer than in the meta isomer with these molecules as well. The results presented above suggest that singlet–singlet transfer here may also be mediated by interactions of the π-electrons of the aryl group with those of the porphyrin macrocycle. Singlet–singlet energy transfer by an electron-exchange mechanism which may involve the linkage bonds has been reported with other types of bichromophoric molecules.[69-71]

If S_1 is the donor state for singlet energy transfer, then one can imagine an interesting relationship between the evolution of singlet and triplet energy transfer processes in natural photosynthesis.[25] Due to its electric dipole forbidden nature, S_1 as an energy donor mimics a triplet state. As a consequence, in order for the carotenoid to function as an antenna to chlorophyll, the evolution of a protein structure which brought the pigments into an arrangement which provided orbital contact was necessary. Although this evolution would have occurred in preoxygenic times, it would set the stage for triplet energy transfer from chlorophyll to carotenoid and in so doing endow a photoprotective carotenoid function. Photoprotection in turn has made possible the evolution of green plants, an oxygenic atmosphere, and life forms in which oxygen is the terminal electron acceptor.

If singlet–singlet energy transfer occurs from the S_2 state of the carotenoid, then the Förster treatment comes much closer to rationalizing the observed rates. If one were to "tune" the conformations of **1–3** to achieve certain combinations of κ^2 and R_{cc}, it would most likely be possible to reproduce the trend shown in Figure 15. On the other hand, singlet–singlet energy transfer from the S_2 state to the porphyrin could also in principle occur via an exchange mechanism. A first step toward resolving this problem would be to determine the nature of the carotenoid donor state in **1–3** using subpicosecond transient absorption spectroscopy.

In summary, the partially conjugated amide linkage in molecules such as **1–5** and a large number of other multicomponent molecular mimics of photosynthesis plays an important role in electron, triplet energy, and probably singlet energy transfer. This can be rationalized in terms of a superexchange pathway involving the π-electrons of the linker. This information should facilitate the design of new artificial reaction centers and related photochemically active species.

Experimental Section

Spectroscopic Measurements. The ^1H NMR spectra were obtained at 300 or 500 MHz and used ≤1% solutions in chloroform-*d* with tetramethylsilane as an internal reference. The UV–vis spectra were recorded on a Hewlett–Packard 8450A spectrophotometer. For transient absorption studies, samples were placed in 1 cm × 1 cm × 4 cm cuvettes and deoxygenated by bubbling with argon. The apparatus used for the transient absorption work features excitation with ca. 15-ns pulses of less than 1 mJ at 590 nm. An adequate signal-to-noise ratio was achieved by signal averaging (typically for about 500 flashes). The details of the spectrometer have been described elsewhere.[72,73] Fluorescence decay measurements were made on ca. 1×10^{-5} M solutions using the time-correlated single photon counting method. The excitation source was a frequency-doubled, mode-locked Nd-YAG laser coupled to a synchronously pumped, cavity dumped dye laser with excitation at 590 nm. Detection was via a microchannel plate photomultiplier (Hamamatsu R2809U-01), and the instrument response time was ca. 35 ps.[74]

Carotenoids **7**[13] and **8**[29] have been previously reported. Carotenoporphyrins **1–3** have been previously discussed,[24] but their syntheses have not been reported.

5-(3-Aminophenyl)-10,15,20-tris(4-methylphenyl)porphyrin. To a 1-L flask equipped with a mechanical stirrer, condenser, and addition funnel were added 300 mL of propionic acid, 22.54 g (0.188 mol) of *p*-tolualdehyde, and 11.3 g (0.075 mol) of *m*-nitrobenzaldehyde. The pale yellow solution was brought to reflux, and 16.77 g (0.25 mol) of pyrrole was added as rapidly as possible, without causing overheating. Refluxing was continued for an additional 40 min. After cooling, the mixture was filtered, and the solid porphyrin mixture was washed with cold methanol until the filtrate was free of brown tar. After the remaining solid was dried, it (5.0 g) was dissolved in 150 mL of concentrated hydrochloric acid to which was added 10 g of stannous chloride dihydrate. The resulting green suspension was allowed to react for 40 min at 70 °C, cooled, and treated with concentrated aqueous ammonia until a pH of 8 was obtained. The solution was then extracted several times with chloroform, and the combined organic extracts were washed with three 300-mL portions of 10% aqueous ammonia and then two 400-mL portions of water. The solution containing the mixture of aminoporphyrins was dried over sodium sulfate. In order to simplify the purification process, the mixture of porphyrins was converted to the *N*-acetyl form. The mixture was first dissolved in a solution of 400 mL of chloroform, 30 mL of pyridine, and 20 mL of acetic anhydride and allowed to stir at room temperature under a nitrogen atmosphere for 7 h. The solvent was then evaporated at reduced pressure, and residual pyridine and acetic anhydride were removed by azeotropic distillation with a 200-mL portion of toluene. The residue was dissolved in chloroform and washed with aqueous citric acid and aqueous sodium bicarbonate, and the solution was dried with sodium sulfate. Evaporation of the solvent at reduced pressure gave a purple solid, which was purified by column chromatography (silica gel/chloroform containing up to 2% acetone). The desired *N*-acetylporphyrin was collected, dissolved in chloroform, and refluxed for 30 min with 0.8 g of 2,3-dichloro-5,6-dicyanobenzoquinone to remove chlorins. After cooling, the solution was passed through a short bed of alumina to remove excess and reduced quinone. The eluate was evaporated to dryness at reduced pressure, and the residue was treated with 250 mL of concentrated hydrochloric acid for 19 h at 80 °C to hydrolyze the amide functionality. The green reaction mixture was cooled and neutralized with aqueous sodium hydroxide, and the reddish product was extracted with dichloromethane and recrystallized from dichloromethane/methanol to give 1.18 g of the desired porphyrin (2.8% yield): ^1H NMR (300 MHz, $CDCl_3$) δ −2.78 (2 H, s, pyrrole NH), 2.69 (9 H, s, tolyl CH_3), 7.04–7.63 (4 H, m, 5ArH), 7.54 (6 H, d, J = 8.0 Hz, 10,15,20ArH), 8.09 (6 H, d, J = 8.0 Hz, 10,15,20ArH), 8.85–8.94 (8 H, m, pyrrole H); mass spectrum (EI) m/z 671 (M^+); UV–vis (dichloromethane) λ_{max} (nm) 420, 518, 552, 592, 648.

5-(2-Aminophenyl)-10,15,20-tris(4-methylphenyl)porphyrin was prepared using the method described above for the 3-aminophenyl analogue to give a 1.6% yield of the desired porphyrin: ^1H NMR (300 MHz, $CDCl_3$) δ −2.74 (2 H, s, pyrrole NH), 2.70 (9 H, s, tolyl CH_3), 7.09–7.90 (5 H, m, 5ArH), 7.55 (6 H, d, J = 7.8 Hz, 10,15,20ArH), 8.09 (6 H, d, J = 7.8 Hz, 10,15,20ArH), 8.86–8.88 (8 H, m, pyrrole H); mass spectrum (EI) m/z 671 (M^+); UV–vis (dichloromethane) λ_{max} (nm) 418, 516, 552, 592, 648.

Carotenoporphyrin 1. To a 50-mL flask were added 70 mg (0.01 mmol) of 7′-apo-7′-(4-carboxyphenyl)-β-carotene,[13] 20 mL of dry benzene, 29 μL (0.40 mmol) of thionyl chloride, and 80 μL (0.99 mmol) of dry pyridine. The initial orange suspension was rapidly converted into the acid chloride as indicated by a dark red color. After the solution was stirred for 30 min under argon, the solvent was distilled under vacuum. Benzene (40 mL) was added and evaporated to dryness under vacuum to remove excess thionyl chloride. The residue that remained was dissolved in 30 mL of dry dichloromethane and added to a solution of 133 mg (0.198 mmol) of 5-(4-aminophenyl)-10,15,20-tris(4-methylphenyl)-porphyrin[13] which was dissolved in 60 mL of dry dichloromethane and 0.2 mL of dry pyridine. This solution was stirred under argon for 60 min and then partitioned between dichloromethane and water. The organic layer was washed twice with 70-mL portions of water, the solvent was evaporated, and the residue was dried under vacuum. Chromatography on silica gel with toluene/0.5% ethyl acetate as the solvent and subsequent recrystallization from methylene chloride/methanol gave 82 mg (53% yield) of the carotenoporphyrin **1**: ^1H NMR (400 MHz, $CDCl_3$) δ 1.05 (6 H, s, C16, C17), 1.48 (2 H, m, C2), 1.62 (2 H, m, C3), 1.73 (3 H, s, C18), 1.99–2.04 (11 H, m, C19, C20, C20′, C4), 2.09 (3 H, s, C19′), 2.71 (9 H, s, tolyl CH_3), 6.0–7.1 (14 H, m, vinyl H), 7.55 (6 H, d, J = 5.9 Hz, 10,15,20Ar3,5H), 7.61 (2 H, d, J = 6.4 Hz, C2′, C4′), 7.98 (2 H, d, J = 6.4 Hz, C1′, C5′), 8.03 (2 H, d, J = 6.6 Hz, 5Ar3,5H), 8.06 (6 H, d, J = 6.1 Hz, 10,15,20Ar2,6H), 8.15 (1 H, s, NH), 8.22 (2 H, d, J = 6.6 Hz, 5Ar2,6H), 8.87 (8 H, m, pyrrole H); UV–vis (dichloromethane) λ_{max} (nm) 376, 418, 480, 512, 550 (sh), 590, 648.

Carotenoporphyrin 2 was prepared as described above for **1** using 133 mg (0.198 mmol) 5-(3-aminophenyl)-10,15,20-tris(4-methylphenyl)-porphyrin to give 79 mg (51%) of product: ^1H NMR (500 MHz, $CDCl_3$) δ 1.04 (6 H, m, C16, C17), 1.48 (2 H, m, C2), 1.63 (2 H, m, C3), 1.73 (3 H, s, C18), 1.98 (9 H, s, C19, C20, C20′), 2.02 (3 H, s, C19′),

(69) See, for example, refs 44, 70, and 71.
(70) Hassoon, S.; Lustig, H.; Rubin, M. B.; Speiser, S. *J. Phys. Chem.* **1984**, *88*, 6367.
(71) Kroon, J.; Oliver, A. M.; Paddon-Row, M. N.; Verhoeven, J. W. *J. Am. Chem. Soc.* **1990**, *112*, 4868.
(72) Gust, D.; Moore, T. A.; Makings, L. R.; Liddell, P. A.; Nemeth, G. A.; Moore, A. L. *J. Am. Chem. Soc.* **1986**, *108*, 8028.
(73) Davis, F. S.; Nemeth, G. A.; Anjo, D. M.; Makings, L. R.; Gust, D.; Moore, T. A. *Rev. Sci. Instrum.* **1987**, *58*, 1629.
(74) Gust, D.; Moore, T. A.; Luttrull, D. K.; Seely, G. R.; Bittersmann, E.; Bensasson, R. V.; Rougée, M.; Land, E. J.; De Schryver, F. C.; Van der Auweraer, M. *Photochem. Photobiol.* **1990**, *51*, 419.

2.70–2.71 (9 H, m, tolyl CH_3), 6.0–7.0 (14 H, m, vinyl H), 7.44 and 7.83 (4 H, AB, C1′, C5′, C2′, C4′), 7.55 (6 H, m, 10,15,20Ar3,5H), 8.85 (8 H, m, pyrrole H); UV–vis (dichloromethane) λ_{max} (nm) 373, 418, 512, 550 (sh), 590, 646.

Carotenoporphyrin 3 was prepared as described above for **1** using 133 mg (0.198 mmol) of 5-(2-aminophenyl)-10,15,20-tris(4-methylphenyl)-porphyrin to yield 49 mg (32%) of the desired product: ^{1}H NMR (400 MHz, $CDCl_3$) δ 1.02–1.06 (6 H, m, C16, C17), 1.48 (2 H, m, C2), 1.62 (2 H, m, C3), 1.72 (3 H, s, C18), 1.87 (3 H, s, C19′), 1.96–1.98 (9 H, s, C19, C20, C20′), 2.0 (2 H, m, C4), 2.70–2.72 (9 H, m, tolyl CH_3), 5.90–6.90 (14 H, m, vinyl H), 6.43 and 6.49 (4 H, AB, J = 8.5 Hz, ArH), 7.50–8.20 (12 H, m, ArH), 8.80–9.10 (8 H, m, pyrrole H); UV–vis (dichloromethane) λ_{max} (nm) 373, 418, 480, 512, 550 (sh), 590, 648.

7′-Apo-7′-(4-aminophenyl)-β-carotene. To a 100-mL flask were added 0.50 g (1.2 mmol) of 8′-apo-β-carotenal, 80 mL of dimethyl sulfoxide, 1.1 g (2.4 mmol) of [4-(*N*-acetylamino)benzyl]triphenylphosphonium bromide, and 0.20 g (3.7 mmol) of sodium methoxide. The mixture was stirred for 5 h under argon at 60–70 °C and was then quenched by pouring the dark orange solution into 500 mL of ether and washing the resulting solution with water repeatedly in order to remove most of the dimethyl sulfoxide. The organic layer was dried over anhydrous magnesium sulfate and filtered, and the solvent was evaporated under reduced pressure. The resulting crude carotenoid amide was dissolved in 30 mL of tetrahydrofuran to which 75 mL of saturated methanolic potassium hydroxide solution was added. This solution was heated to 63 °C, stirred under an argon atmosphere for 5.5 h, and then poured into 500 mL of ether and washed six times with 150-mL portions of water. The organic layer was dried over anhydrous magnesium sulfate and filtered, and the solvent was evaporated. The residue was chromatographed with chloroform on a dry-packed silica gel column to give 319 mg (53% yield) of the pure aminocarotenoid: ^{1}H NMR (400 MHz, $CDCl_3$) δ 1.03 (6 H, s, C16, C17), 1.48 (2 H, m, C2), 1.61 (2 H, m, C3), 1.72 (3 H, s, C19′), 1.97–1.98 (9 H, m, C19, C20, C20′), 2.00 (2 H, m, C4), 2.02 (3 H, s, C19′), 3.75 (2 H, s, NH_2), 6.11–6.76 (14 H, m, vinyl H), 7.25–7.28 (4 H, m, ArH); mass spectrum (EI) m/z 506 (M^+); UV–vis (dichloromethane) λ_{max} (nm) 376, 478, 506.

Carotenoporphyrin 4. To a 50-mL flask equipped with a condenser and nitrogen gas line were added 120 mg (0.171 mmol) of 5-(4-carboxyphenyl)-10,15,20-tris(4-methylphenyl)porphyrin,[75] 30 mL of dichloromethane, and 3.0 mL of oxalyl chloride. The dark green solution was refluxed under nitrogen for 1 h and cooled, and the solvent was evaporated under vacuum. Two 25-mL portions of toluene were successively added and then evaporated under vacuum in order to remove all traces of excess oxalyl chloride. The residue was dissolved in a mixture of dichloromethane (50 mL) and pyridine (1 mL). The resulting solution was added to 70 mg (0.138 mmol) of 7′-apo-7′-(4-aminophenyl)-β-carotene dissolved in 50 mL of dichloromethane and stirred under argon. After 1 h, the reaction mixture was poured into 180 mL of dichloromethane and washed twice with 100-mL portions of water. The organic layer was separated, and the solvent was evaporated. Residual water and pyridine were removed by azeotropic distillation with toluene. The residue was chromatographed on silica gel (dichloromethane), and the product was recrystallized from dichloromethane/methanol to afford 76 mg (46% yield) of the pure carotenoporphyrin **4**: ^{1}H NMR (400 MHz, $CDCl_3$) δ 1.03 (6 H, m, C16, C17), 1.47 (2 H, m, C2), 1.62 (2 H, m, C3), 1.72 (3 H, s, C18), 1.98–2.01 (9 H, m, C19, C20, C20′), 2.02–2.06 (2 H, m, C4′), 2.08 (3 H, s, C19′), 2.71 (9 H, s, tolyl CH_3), 6.0–7.0 (14 H, m, vinyl H), 7.52–7.60 (8 H, m, 10,15,20Ar3,5H and C2′, C4′), 7.77 (2 H, d, J = 8.6 Hz, C1′, C5′), 8.10 (6 H, d, J = 7.9 Hz, 10,15,20Ar2,6H), 8.14 (1 H, s, NH), 8.26 and 8.35 (4 H, AB, J = 8.2 Hz, 5ArH), 8.78–9.00 (8 H, m, pyrrole H); UV–vis (dichloromethane) λ_{max} (nm) 373, 418, 476, 510, 550 (sh), 592, 648.

Carotenoporphyrin 5 was prepared by a method similar to that described for **4** from 100 mg (0.143 mmol) of 5-(2-carboxyphenyl)-10,15,20-tris(4-methylphenyl)porphyrin (prepared by hydrolysis[75] of the corresponding carbomethoxy-substituted porphyrin[76]). A total of 77 mg of pure product was obtained (45% yield): ^{1}H NMR (400 MHz, $CDCl_3$) δ 1.02–1.05 (6 H, m, C16, C17), 1.47 (2 H, m, C2), 1.60 (2 H, m, C3), 1.69 (3 H, s, C18), 1.71 (3 H, s, C19′), 1.86 (3 H, s, C20′), 1.95–1.97 (6 H, m, C19, C20), 2.01–2.05 (2 H, m, C4), 2.70 (9 H, s, tolyl CH_3), 5.50–6.80 (14 H, m, vinyl H), 7.03 (1 H, s, NH), 7.50–8.50 (20 H, m, aromatic H), 8.77–8.91 (8 H, m, pyrrole H); UV–vis (dichloromethane) λ_{max} (nm) 372, 418, 478, 512, 550 (sh), 592, 648.

Porphyrin 6. To a 100-mL flask were added 110 mg (0.16 mmol) of 5-(4-aminophenyl)-10,15,20-tris(4-methylphenyl)porphyrin,[13] 40 mL of dichloromethane, and 40 μL (0.49 mmol) of pyridine. The mixture was stirred under a nitrogen atmosphere, and 37 μL (0.32 mmol) of benzoyl chloride was added. The reaction was complete after 30 min. The mixture was diluted with 60 mL of dichloromethane and washed with dilute hydrochloric acid, aqueous sodium bicarbonate, and aqueous sodium chloride. The resulting organic phase was dried over anhydrous sodium sulfate and filtered, and the solvent was distilled from the filtrate under reduced pressure. The resulting purple solid was recrystallized from dichloromethane/methanol to give 115 mg (92% yield) of the desired porphyrin: ^{1}H NMR (300 MHz, $CDCl_3$) δ −2.77 (2 H, s, pyrrole NH), 2.71 (9 H, s, tolyl CH_3), 7.56 (6 H, d, J = 7.9 Hz, 10,15,20ArH), 7.60–8.07 (5 H, m, ArH), 8.05 (2 H, d, J = 8.3 Hz, 5ArH), 8.10 (6 H, d, J = 7.9 Hz, 10,15,20ArH), 8.16 (1 H, s, NH), 8.24 (2 H, d, J = 8.3 Hz, 5ArH), 8.87–8.88 (8 H, m, pyrrole H); mass spectrum (EI) m/z 775 (M^+); UV–vis (dichloromethane) λ_{max} (nm) 420, 518, 554, 594, 650.

Acknowledgment. This research was supported by the National Science Foundation (CHE-8903216, BBS-8804992) and the Department of Energy University Research Instrumentation Program (DE-FG05-87ER75361). This is publication no. 97 from the Arizona State University Center for the Study of Early Events in Photosynthesis. The Center is funded by U.S. Department of Energy Grant DE-FG02-88ER13969 as part of the U.S. Department of Agriculture–Department of Energy–National Science Foundation Plant Science Center Program.

Registry No. 1, 110390-86-8; **1** (R_1 = R_2 = H; R_3 = NH_2), 73170-32-8; **2**, 139656-11-4; **2** (R_1 = R_3 = H; R_2 = NO_2), 139656-14-7; **2** (R_1 = R_3 = H; R_2 = NH_2), 78265-41-5; **3**, 139656-12-5; **3** (R_2 = R_3 = H; R_1 = NH_2), 131352-79-9; **4**, 139703-77-8; **4** (R_1 = R_2 = H; R_3 = CO_2H), 61449-63-6; **5**, 139687-85-7; **5** (R_2 = R_3 = H; R_1 = CO_2H), 78265-42-6; **6**, 139656-13-6; *p*-tolualdehyde, 104-87-0; *m*-nitrobenzaldehyde, 99-61-6; pyrrole, 109-97-7; 7′-apo-7′-(4-carboxyphenyl)-β-carotene, 90447-13-5; 8′-apo-β-carotenal, 1107-26-2; [4-(acetylamino)-benzyl]triphenylphosphonium bromide, 139656-15-8; 7′-apo-7′-(4-aminophenyl)-β-carotene, 103563-96-8.

(75) Anton, J. A.; Kwong, J.; Loach, P. A. *J. Heterocycl. Chem.* **1976**, *13*, 717.

(76) Anton, J. A.; Loach, P. A. *J. Heterocycl. Chem.* **1975**, *12*, 573.

(77) We thank Professor R. Fessenden for allowing us to make this measurement using his spectrometer.